UNIVERSITÉ DE MONTRÉAL

INTEGRATED OPTICS WDM AND POWER SPLITTER IN GLASS

par

Guangwen ZHANG

DÉPARTEMENT DE GÉNIE PHYSIQUE

ÉCOLE POLYTECHNIQUE

MÉMOIRE PRÉSENTÉ EN VUE DE L'OBTENTION

DU GRADE DE MAÎTRE ES SCIENCES APPLIQUÉES (M.Sc.A.)

(GÉNIE PHYSIQUE)

mars 1994

Refusée

par la BNC

UNIVERSITÉ DE MONTRÉAL

ÉCOLE POLYTECHNIQUE

Ce mémoire intitulé :

INTEGRATED OPTICS WDM
AND POWER SPLITTER IN GLASS

présenté par: Guangwen ZHANG

en vue de l'obtention du grade de: MAÎTRE ÈS SCIENCES APPLIQUÉES (M.Sc.A.)

a été dûment accepté par le jury d'examen constitué de:

M. MARTINU Ludvik, Ph.D., président

M. NAJAFI, S. Iraj, Ph.D., membre et directeur de recherche

M. SCHWELB Otto Schwelb, Ph.D., membre

SOMMAIRE

Cette recherche porte sur divers composants en optique intégrée sur verre. Plus particulièrement, les caractéristiques de multi/démultiplexeurs (WDM) ainsi que celles de diviseurs de puissance sont étudiées.

Un procédé conventionnel de photolithographie ainsi que la technique de l'échange ionique double (ions de potassium et d'argent) sont mis à profit pour fabriquer ces composants passifs de haute performance qui sont, par exemple, nécessaires dans le domaine des télécommunications.

L'intégration sur un même substrat de verre d'un multiplexeur (1,30 et 1,55 μm) et d'un diviseur de puissance un pour huit est analysée. Ce composant est constitué en premier lieu d'un interféromètre Mach-Zehnder asymétrique pour le multiplexage des deux longueurs d'onde. En second lieu, la division en puissance du signal est faite de façon achromatique par des jonctions Y symétriques.

Les effets d'un recuit thermique sur la réponse spectrale d'un multi/démultiplexeur 1,30/1,55 μm et d'un autre 1,48/1,55 μm sont étudiés. Il a été observé que pour le premier composant, en l'occurrence l'interféromètre 1,30/1,55 μm, cette réponse ne dépend pas du recuit tandis que celle du second composant changera.

L'intégration de multi/démultiplexeur 1,48/1,55 μm seul

et celle d'un multi/démultiplexeur 1,30/1,55 μm suivi par un diviseur de puissance un pour huit sur un même substrat de verre est démontrée. Les pertes en surplus entre la face d'entrée et de sortie sont, dans les deux cas (interféromètre 1,48/1,55 μm seul et interféromètre 1,30/1,55 μm avec diviseur de puissance), inférieures à 2.7 dB. Ce dernier composant pourrait être utilisé dans de futurs réseaux où l'amplification des signaux à 1,55 μm est nécessaire.

ABSTRACT

The characteristics of integrated optical wavelength division multiplexer (WDM) and demultiplexer, and power splitters in glass are studied.

The conventional photolithography and double-ion exchange (K^+ and Ag^+) processes are used to fabricate high performance passive devices, which are needed in telecommunication and Cable (CATV) subscriber networks.

Integration of a 1.30/1.55 μm WDM and a 1/8 splitter in a single glass substrate is demonstrated. The device is composed of a nonsymmetric Mach-Zehnder interferometer for wavelength multiplexing, and symmetric Y-branches for achromatic splitting.

The effect of thermal post-annealing on spectral behaviour of the 1.30/1.55 μm and 1.48/1.55 μm WDM is investigated. It is observed that the spectral transmission of the 1.30/1.55 μm device is not sensitive to post-annealing while that of the 1.48/1.55 μm device changes after post-annealing.

The integration of a 1.48/1.55 μm WDM, and a 1.30/1.55 μm WDM followed by a 1/8 splitter in a single glass substrate is demonstrated. The facet to facet excess loss both in the 1.48/1.55 μm WDM and in the integrated 1.30/1.55 μm WDM and 1/8 splitter is less than 2.7 dB. The device can be used in future WDM subscriber networks, in which amplification is needed in the 1.55 μm wavelength region.

RÉSUMÉ

Le domaine de l'optique intégrée repose essentiellement sur des phénomènes physiques survenant lors du transport d'une onde électromagnétique à fréquence optique à travers des structures faites de couches minces. L'optique intégrée couvre ainsi tout ce qui concerne les circuits optiques miniaturisés. Les composante de ces circuits intégrés peuvent être classées selon trois catégories différentes, soient les composants passives, dynamiques et actifs. Les guides d'onde sont des composants passifs, et constituent la base de l'optique intégrée. Le travail présenté dans ce mémoire concerne principalement des composants passifs.

Les composants optiques, dont les guides d'onde, peuvent être fabriquées sur différents substrats en utilisant diverses méthodes. Le verre est un substrat qui s'avère très intéressant pour les applications en optique intégrée. Dans ce travail, des dispositifs sont fabriqués dans le verre en utilisant une technique d'échange ionique double avec des ions de potassium et des ions d'argent. Les guides d'onde produits par cette méthode ont à la fois les qualités des guides d'onde fabriqués par l'échange ionique du potassium et celles des guides d'onde fabriqués par l'échange ionique d'argent. Ce sont donc des guides d'onde permettant un bon confinement de mode, offrant peu de pertes par propagation et ayant une absorption faible dans le visible. Les dispositifs étudiés

dans ce travail sont les suivants: 1) des jonctions Y symétriques, 2) des jonctions Y asymétriques, 3) des interféromètres de type Mach-Zehnder et 4) des multi/démultiplexeurs (WDM).

Les fibres optiques sont de plus en plus employées dans le domaine des télécommunications, ce qui exige l'utilisation de composants passifs de grande qualité, telles que des diviseurs de puissance 1/N agissant sur une large plage de longueurs d'onde, ou des coupleurs sélectifs de longueurs d'onde pour le WDM. Les divisions successives du signal lumineux dans ces réseaux exige également l'emploi d'amplificateurs afin de pallier à la diminution de la puissance du signal. On peut introduire de tels amplificateurs, agissant à la longueur d'onde de 1.55 μm, simplement en dopant des guides d'onde avec de l'erbium (Er). Ces amplificateurs nécessitent l'utilisation de composants WDM permettant le multiplexage de la longueur d'onde de pompage (1.48 μm) à celle du signal (1.55 μm).

Les caractéristiques des composants d'optique intégrée répondent bien aux critères de qualité requis pour les applications en telecommunication. De plus, ces composants peuvent être facilement fabriqués à une échelle industrielle. Toutefois, pour tirer le plus de profit de l'optique intégrée, il faudrait intégrer sur un même substrat plusieurs composants, ce qui augmenterait la fiabilité des circuits tout en réduisant les coûts reliés aux interconnexions avec des de fibres optiques et à l'encapsulation des circuits.

Dans cette thèse, un multi/démultiplexeur 1.48/1.55 μm, un multi/démultiplexeur 1.30/1.55 μm et un diviseur de puissance 1/8 sont intégrés sur un même substrat de verre. Les performances de ce dispositif WDM/diviseur de puissance sont démontrées.

Au chapitre 2, un dispositif WDM 1.30/1.55 μm et diviseur de puissance 1/8 fabriqué sur un substrat de verre sont décrits et analysés. Les pertes en surplus entre la face d'entrée et la face de sortie du dispositif (long de 40 mm) sont inférieures à 2.5 dB et ce, malgré le fait que nous avons utilisé un masque d'aluminium lors de l'échange ionique ainsi qu'un substrat de verre de qualité moyenne. La déviation du signal aux huit branches de sortie est faible.

Le chapitre 3 présente en détail la caractérisation optique d'un dispositif multi/démultiplexeur à 3 banches intégrant des interféromètres Mach-Zehnder 1.30/1.55 μm et 1.48/1.55 μm sur un même substrat de verre. En particulier, l'effet d'un recuit sur les propriétés optiques fait l'objet d'une étude détaillée. Dans l'ensemble, les caractéristiques spectrales du dispositif 1.30/1.55 μm sont peu affectées par un recuit. La longueur d'onde centrale de la bande d'arrêt demeure inchangée. Comme les guides d'onde fabriqués sont en régime multimode autour de 1.30 μm, il se produit quelques oscillations dans le spectre de transmission. Le recuit accroît les performances du dispositif et augmente le rapport d'extinction à cette longueur d'onde puisque plus de lumière venant de la fibre est couplée dans le mode fondamental (dont le profil est devenu plus large). Le rapport d'extinction obtenu n'est pas très grand puisque la longueur d'onde à laquelle la mesure est prise est proche de la longueur d'onde centrale de la bande d'arrêt. A 1.55 μm, le rapport d'extinction diminue puisque le guide d'onde entre en régime bi-modal après un long recuit. Pour éliminer complètement cet effet, des guides d'onde avec de grandes parties monomode doivent être fabriqués. Ceci peut être fait, par exemple, en enterrant les guides d'onde.

En ce qui concerne les caractéristiques spectrales des dispositifs 1.48/1.55 μm, celles-ci sont plus affectées par les recuits. Ceci était prévisible du fait de la plus grande différence de longueur entre les trajets des deux bras de l'interféromètre et aussi à cause du petit rayon de courbure. Cet effet peut être mis à profit lors de la fabrication de dispositifs puisqu'une grande précision est requise lorsque l'espacement entre longueurs d'onde est faible. Le recuit peut être utilisé pour faire un ajustement fin des caractéristiques spectrales des dispositifs une fois la fabrication complétée. Les dispositifs passifs fabriqués peuvent être employés de pair avec une fibre dopée à l'erbium dans de futurs réseaux WDM exigeant une amplification à 1.55 μm. Un dispositif similaire peut être fait pour 1.30 μm (0.807/1.30 μm si des fibres dopées au Nd sont utilisées). Le dispositif 1.30/1.55

μm peut être employé pour le multiplexage de deux signaux amplifiés. Il peut aussi être utilisé lorsque le démultiplexage de ces signaux est requis.

Au chapitre 4, nous étudions un circuit d'optique intégrée sur verre composé d'un multiplexeur 1.48/1.55 μm, et d'un multiplexeur 1.30/1.55 μm suivi d'un diviseur de puissance 1/8. Les pertes en surplus entre les faces d'entrée et de sortie du dispositif (40 mm de long) sont inférieures à 2.49 dB pour le multiplexeur 1.48/1.55 μm et inférieures à 2.65 dB pour le multiplexeur 1.30/1.55 μm et le diviseur de puissance et ce, malgré l'utilisation d'un masque d'aluminium lors de l'échange ionique et d'un substrat de verre de qualité moyenne. Ce circuit peut être utilisé avec une fibre dopée à l'erbium dans de futurs dispositifs WDM demandant une amplification de la lumière autour de 1.55 μm.

Tout au long de ce travail, nous avons utilisé des guides d'onde fabriqués à la surface de substrats de verre par double échange ionique. Ces guides ont un intervalle spectral d'opération en régime monomode relativement étroit. En fait, les guides d'onde ne sont clairement monomode qu'à 1.55 μm seulement et quasi-monomode à 1.48 μm. Dans la région spectrale autour de 1.30 μm, les guides d'onde supportent plusieurs modes. Dans le cas étudié ici, ce fait ne cause pas de problèmes puisque des fibres monomode sont utilisées à l'entrée des multiplexeurs, assurant ainsi l'opération du dispositif dans le mode fondamental. Cependant, dans un système WDM bidirectionnel, le multiplexeur 1.30/1.55 μm devrait aussi agir comme un multiplexeur. Dans ce cas, si un signal à 1.30 μm est transmis par le dispositif, les guides d'onde devraient être monomode à 1.30 μm, sinon la performance du démultiplexeur 1.30/1.55 μm sera altérée par les modes d'ordres supérieurs excités dans le combineur de puissance qu'est la jonction Y. Toutefois, il serait aisé de faire le design de notre dispositif en utilisant de guides d'onde sous la surface du verre, lesquels sont monomode à 1.30 μm et à 1.55 μm.

ACKNOWLEDGMENTS

The author wishes to express his sincere appreciation to Professor S. Iraj Najafi for his guidance and invaluable help during the experiments and the course of study.

Special thanks is to Dr. Seppo Honkanen for his patient help, valuable discussions and suggestions.

The author would like to acknowledge the valuable contribution of Dr. Ari Terronen of Optonex to the design of the devices in this project.

The author wishes to thank his colleagues: Jianyao Chen, Pierre L.-Auger, Qing He, Paul Lefebvre, Sylvain Lafrenière, and Véronique François for their various helpful suggestions.

The author is indebted to his parents and all family for all that they have done to support him in all his endeavour.

The author would also express his appreciation to his wife, Li Li, for her love, understanding, encouragement and support.

TABLE OF CONTENTS

SOMMAIRE iv

ABSTRACT vi

RÉSUMÉ vii

ACKNOWLEDGEMENTS xiii

TABLE OF CONTENTS xiv

LIST OF FIGURES xvii

LIST OF TABLES xix

CHAPTER 1 INTRODUCTION 1

1.1 Integrated Optics 2

1.2 Glass Integrated Optics 3

1.3 Ion-Exchanged Glass Waveguides 4

1.4 Double Ion-Exchanged Waveguides 6

1.5 Theoretical Analysis 8

1.6 Passive Glass Waveguide Devices 12

1.7 References 22

CHAPTER 2 INTEGRATED 1.30/1.55 μm WAVELENGTH MULTIPLEXER AND 1/8 SPLITTER BY ION EXCHANGE IN GLASS 25

2.1 Introduction 27

2.2 Device Operation and Design 29

2.3 Fabrication 30

2.4 Measurements 31

2.5 Conclusion 34

2.6 Acknowledgement 35

2.7 References 36

CHAPTER 3 ION-EXCHANGED GLASS WAVEGUIDE MACH-ZEHNDER INTERFEROMETERS FOR WAVELENGTH MULTI/DEMULTIPLEXING AND THE EFFECT OF THERMAL POST-ANNEALING ON SPECTRAL TRANSMISSION 38

3.1 Introduction 40

3.2 Mach-Zehnder Interferometer WDM-Devices 41

A. Description 41

B. Design 44

3.3 Fabrication 44

3.4 Measurements and Results 45

3.5 Discussion and Conclusion 51

3.6 Acknowledgment 54

3.7 References 55

CHAPTER 4 GLASS INTEGRATED OPTICS CIRCUIT FOR 1.48/1.55 μm WDM, 1.30/1.55 μm WDM AND 1/8 SPLITTING 57

4.1 Introduction 59

4.2 Device Operation and Design 62

4.3 Fabrication 64

4.4 Measurements 65

4.4.1 1.48/1.55 μm wavelength multiplexer 65

4.4.2 1.30/1.55 μm wavelength multiplexer and 1/8 splitter 67

4.5 Discussion and Conclusion 69

4.6 Acknowledgement 70

4.7 References 72

CHAPTER 5 CONCLUSION 74

REFERENCES 78

LIST OF FIGURES

Figure 1.1 Purely thermal ion exchange process 5

Figure 1.2 Double-ion exchange process 7

Figure 1.3 Fabrication processes 13

Figure 1.4 A schematic diagram of a Mach-Zehnder interferometer 15

Figure 1.5 Microscope photograph of the offset 18

Figure 2.1 A schematic diagram of the integrated wavelength multiplexer and 1/N splitter . . . 28

Figure 2.2 Nearfield photograph of output waveguides of the device (a) at 1.30 μm and (b) at 1.55 μm wavelength 32

Figure 2.3 Measured fibre-chip insertion loss of the device (a) at 1.30 μm and (b) at 1.55 μm wavelength 33

Figure 3.1 A schematic diagram of three-port nonsymmetric Mach-Zehnder interferometer . . 42

Figure 3.2 Measurement setup 47

Figure 3.3 Measured spectral transmission of 1.30/1.55 μm wavelength demultiplexer.
(a) and (b): before post-annealing.
(c) and (d): after post-annealing
(Dotted and solid curves are outputs from

wide and narrow arms, respectively) 49

Figure 3.4 Measured spectral transmission of 1.48/1.55 μm wavelength demultiplexer.
(a) and (b): before post-annealing.
(c) and (d): after post-annealing
(Dotted and solid curves are outputs from wide and narrow arms, respectively) 50

Figure 4.1 A schematic diagram of the studied passive integrated optical circuit in connection with an Er-doped fiber 61

Figure 4.2 Measured spectral transmission of 1.48/1.55 μm wavelength demultiplexer 66

Figure 4.3 Measured fibre-chip insertion loss of the integrated 1.30/1.55 μm wavelength demultiplexer and 1/8 splitter
(a) at 1.273 μm and
(b) at 1.557 μm wavelength 68

LIST OF TABLES

Table 3.1 Device fabrication parameters 46

Table 3.2 Extinction ratio of the fabricated WDMs . . . 52

CHAPTER 1

INTRODUCTION

1.1 Integrated Optics

The term "integrated optics" (IO) was first proposed by Stewart E. Miller [1] in 1969 to describe the optics of miniaturized optical circuits in which light signals are generated, guided and processed by related effects before finally being detected. Integrated optical components are compact and reliable, with high mechanical and thermal stability, and low power consumption. Integrated optics offers the possibility for integration of many devices on a common substrate or chip. During the past 23 years, the development in thin film, microfabrication technology, and optical fibres have made the integrated optical devices become very promising, and they are now in practical uses in the areas of telecommunication, signal processing and sensing [2].

The optical function of an integrated optical component mainly depends on the physical properties of substrate material on which the component is made. Usually, integrated optical components are classified into three categories: passive components, which exhibit fixed optical characteristics for guided waves; dynamic components, which perform dynamic control of guided optical waves; and active components, which generate and amplify optical waves. The typical passive components such as power dividers, polarizers and mode splitters, wavelength division multi/demultiplexers, various static couplers and wavefront sensors are fabricated on a substrate material whose physical properties (like refractive index) can not be changed by an external signal.

In this thesis, the work is mainly on passive optical components.

1.2 Glass Integrated Optics

Glass is an interesting substrate material for integrated optics because of its relatively low cost, excellent transparency, high threshold to optical damage and availability in substantially large sizes. It is also mechanically very rigid. Furthermore, glass substrates are amorphous and it is easier to produce polarization-insensitive components in glass. In addition, refractive index of glasses used in integrated optics (e.g. silicate, phosphate) is close to that of optical fibre and, therefore, coupling losses between the waveguides made in glass and the optical fibres are low.

Integrated optical glass waveguides and passive components can be made by different methods such as radio frequency (RF) sputtering, chemical vapour deposition (CVD), sol gel coating, ion implantation and ion exchange [3].

In this thesis, ion exchange technique is mainly employed for fabrication of passive glass waveguides and devices.

1.3 Ion-Exchanged Glass Waveguides

In the ion-exchange process an ion in glass (usually Na^+) is replaced by an ion of larger size and/or higher polarizability such as Ag^+, K^+, Cs^+ and Tl^+ [3]. Consequently, the refractive index of glass increases locally giving rise to a waveguide. Ion-exchange can be a purely thermal process (see **Figure 1.1**). However, an electrical field may be applied across the substrate to accelerate the process.

Ion-exchange process is suitable for glass waveguide fabrication. This process offers considerable flexibility in the choice of fabrication parameters and, therefore, can be optimized for a wide variety of applications. The process is simple and suitable for high-volume batch processing. The fabricated waveguides are reproducible and have low propagation losses. There is no need for in-situ control of device parameters during the fabrication process due to excellent reproducibility. Waveguides with excellent match to conventional single-mode and multimode fibres can be made, thus minimizing the coupling losses. Ion-exchanged waveguides have a planar configuration. This facilitates considerably the use of other materials (e.g. nonlinear polymers) and devicgw made by using other materials (e.g. detectors) with glass integrated optical devices. Very high performance hybrid

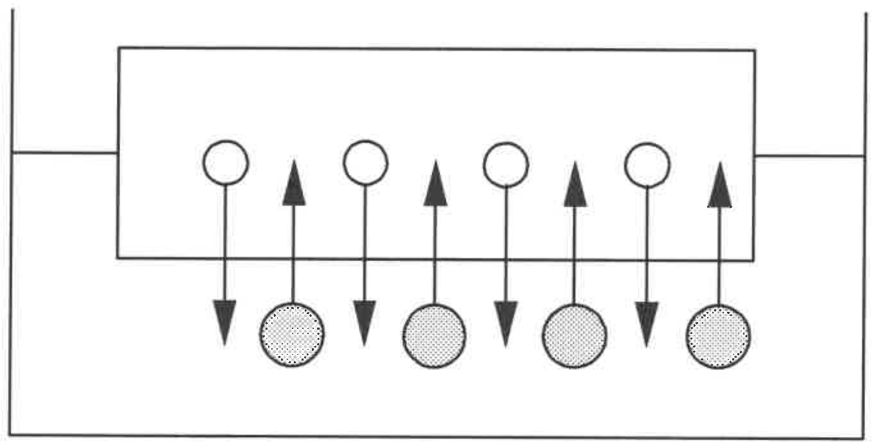

Figure 1.1 Purely thermal ion exchange process

(○ and ◍ represent exchanging ions

in glass and molten salt, respectively)

integrated optical circuits can be achieve in this way.

Ion-exchange process has tremendous potential for fabrication of high performance integrated optics devices. Since fabrication of the first ion-exchanged glass waveguide in 1972 [4], there have been significant progress in this field [3].

1.4 Double Ion-Exchanged Waveguides

In this process, the devices are fabricated by using potassium and silver double-ion-exchange in glass [3]. First, potassium ion exchange carried out using molten pure potassium nitrate. Second, the silver ion exchange is performed in a molten pure silver nitrate bath. Corning 0211 glass substrate is utilized to make the devices. **Figure 1.2** illustrates fabrication of devices by double-ion-exchange process.

Potassium ion-exchange in glass results in a small index increase ($\Delta n = 0.006$). Consequently the waveguides have a large single mode operation regime. The opposite happens in silver ion-exchanged waveguides. Δn is much larger (about 0.09) and, therefore, the waveguides have smaller single mode operation regime. Silver ion-exchanged waveguides absorb considerably light in the visible. This is due to formation of metallic colloids under the metallic mask during ion-exchange process [5]. It results in high propagation losses when these waveguides are operated in the visible. However, in the

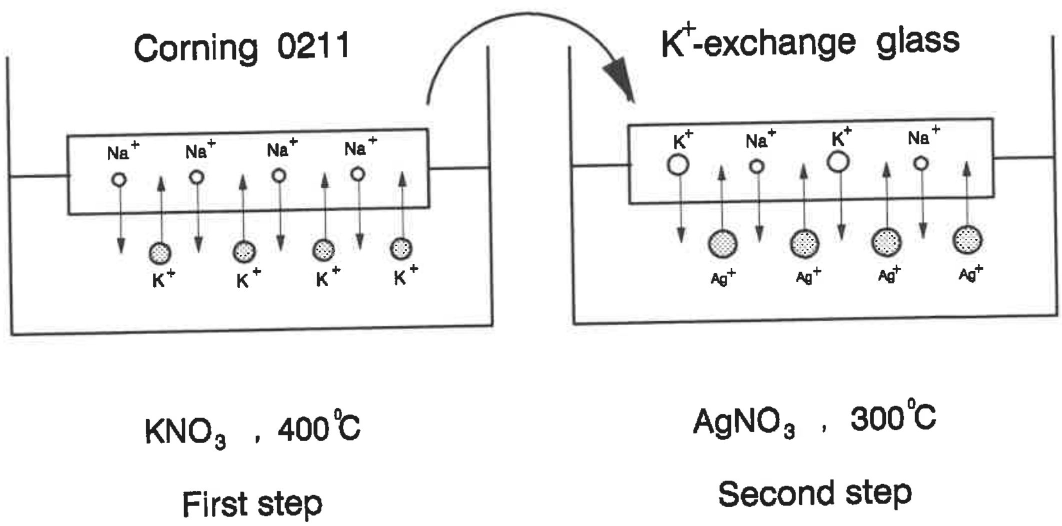

Figure 1.2 Double-ion exchange process

infrared the propagation losses in silver ion-exchanged waveguides are low and they are in the same order of magnitude as those in potassium ion-exchanged waveguides (smaller than 0.2 dB/cm at 1.3 μm) [6].

Absorption in the visible in silver ion-exchanged waveguides can be reduced by using a two-step process. Silver-potassium double ion-exchanged waveguides have essentially the advantages of both silver and potassium single ion-exchanged waveguides: low absorption in the visible, large single-mode regime and good mode confinement. In addition the silver-potassium double ion-exchanged waveguides have a higher damage threshold than single silver ion-exchanged waveguides [7]. Single silver ion-exchanged waveguides break when submitted to high powers possibly because of residual metallic silver forming in the waveguide. Metallic silver formation is reduced in double ion-exchanged waveguides. Single potassium ion-exchanged waveguides have a much greater power handling capability. Single potassium ion-exchange waveguides tolerates at least ten times more power than their silver ion-exchanged counterparts.

1.5 Theoretical Analysis

In order to design the waveguide device, we need to know the waveguides parameters, such as, the refractive index n, the propagation constant ß and the mode profile.

The refractive index profiles of the channel waveguides are directly proportional to the concentration of exchanged ions in the glass substrates. The concentration can be simulated by solving the diffusion equation:

$$\frac{\partial c}{\partial t} = \frac{\partial}{\partial x}\left(D\frac{\partial c}{\partial x}\right) + \frac{\partial}{\partial y}\left(D\frac{\partial c}{\partial y}\right) \tag{1}$$

where c is the relative concentration of the exchanged ions, D is the diffusion coefficient.

Analytic solution for the concentration distribution in channel waveguides does not exist. However, numerical methods can be used to calculate numerically the concentration distribution [3]. The refractive index profile n(x,y) is proportional to the concentration c(x,y) of the exchanged ions [3]. After the concentration c(x,y) is determined, the refractive index profile n(x,y) is obtained as well.

After calculating the refractive index profile, the characteristics of the channel waveguides can be analyzed. A large number of different methods exist for solving the mode propagation constants and field distributions in channel waveguides. More complex methods give the full vector field solutions. However, scalar methods, which make the approximation of taking into account only one field component, are less complicated and faster.

The scalar wave equation:

$$\frac{\partial^2 E}{\partial x^2} + \frac{\partial^2 E}{\partial y^2} - [\beta^2 - (k_0 n(x,y))^2] E = 0 \qquad (2)$$

has the mode solution in the form:

$$E(x,y,z) = E(x,y)\, e^{j(\omega t - \beta z)} \qquad (3)$$

The variational expression for propagation constant, the Rayleigh quotient, for the real part of E gives [3]:

$$\beta^2 = \frac{\iint [\partial^2 E/\partial x^2 + \partial^2 E/\partial y^2 + (k_0 n(x,y))^2 E]\, E\, dxdy}{\iint E^2\, dxdy} \qquad (4)$$

The guided mode field distributions give stationary extreme values for the above equation. In particular, the fundamental mode field distribution maximizes the Rayleigh quotient.

A commercially available software, Ionex [8], is employed to design the ion-exchange waveguides and devices using finite-difference method. This software uses a rectangular grid to calculate the refractive index profile at discrete points. The wave equation (and variational forms derived from it) is also written in finite-difference form for these grid points. A Gaussian field distribution, which maximizes equation 4, is first found for the fundamental mode of the waveguide. From this field distribution the actual field profile of the mode is found by an iterative method. For each iteration step the value of ß is calculated using equation 4. Then the wave equation, written in finite difference form, gives the values of E at the discrete grid points. The calculation is continued until ß is observed to have converged to its maximum value. The result is found in the form of a matrix eigenvalue equation. Solving this matrix equation gives the mode solutions: propagation constants from the eigenvalues and field distributions from the eigenvectors.

When the refractive index distribution, the propagation constants, and the distribution of the input field are determined for the waveguides, the beam propagation method (BPM) is used to design and explore the behaviour of the devices.

In the Mach-Zehnder interferometer, there are straight and curved channel waveguides. When an optical waveguide is bent, the maximum of the mode field shifts away from the waveguide centre towards the core-cladding boundary [9]. This shift in the peak field can cause a radiation loss in the bend and a mode coupling loss with straight waveguide. It is necessary to take into account the mode shift in the field contribution. So, the lateral offsets were designed for bend joints in order to decrease the radiation loss and obtain mode matched coupling.

1.6 Passive Glass Waveguide Devices

A conventional photolithography was used to fabricate the devices. The fabrication process, shown in **Figure 1.3**, includes evaporation, resist spinning, exposure, development, etching, removal of resist, ion exchange and Al mask removal. The ends of the fabricated devices are finally polished.

The devices developed in this work consist of symmetric and asymmetric Y-branches, and Mach-Zehnder interferometers.

Optical waveguide Y-branches are important elements for performing splitting and recombining optical signals in guided-wave devices. Guided-wave Y-branches can be divided into two different categories according to their different application purposes. The first category is asymmetric Y-branches, which have different widths (or different propagation constants) for branching waveguide. They are mainly employed to spatially separate the guided modes in a multimode waveguide [10]. Another category is symmetric Y-branches, which are widely used as power dividers in 1/N branching circuit [11] and in some Mach-Zehnder interferometers [12], and in Y-junction lasers and amplifiers [13]. The symmetric Y-branch exhibits an intrinsic loss of 3 dB as a single mode combiner and divider. The Y-branches are usually employed to divide guided light into two waveguides in an equal ratio. By cascading them, light can be split into 4, 8, 16 or more equal parts. They are utilized in some special

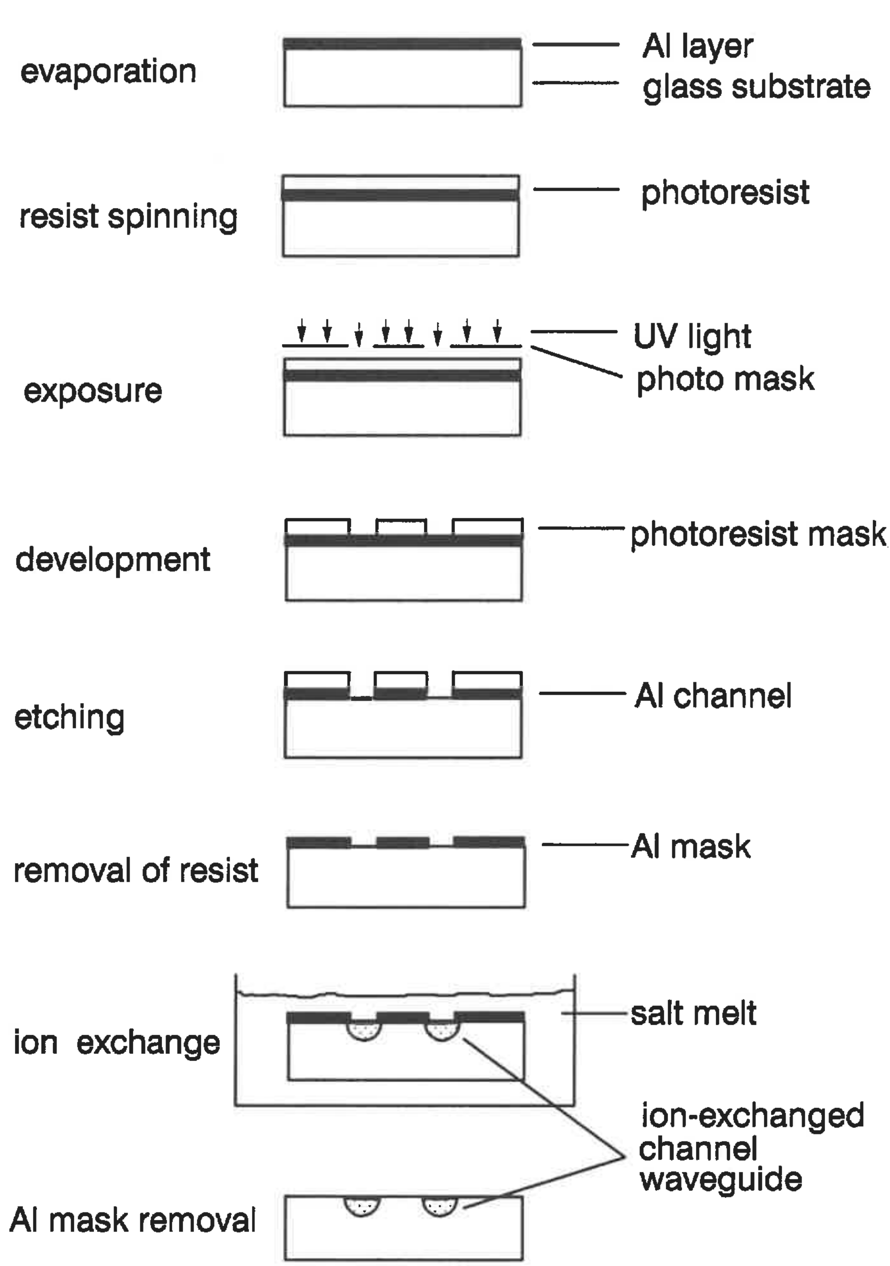

Figure 1.3 Fabrication process

cases such as Mach-Zehnder interferometers as power combiners because the coherence of the combining light can be used to avoid the 3 dB extra loss.

An alternative to the cascaded Y-branch power divides are the computer-generated holographic waveguide (CGHW) beam splitter. A CGWH with fanout to eight beams was fabricated by using potassium and silver double ion-exchange process in Corning 0211 glass. The computer-generated waveguide holograms can have almost arbitrary profiles that would be difficult or virtually impossible to fabricate for free-space optics. They can also be cascaded with a high positional accuracy to build sophisticated diffractive optical systems in planar waveguides [14].

A schematic diagram of a Mach-Zehnder interferometer is shown in **Figure 1.4**. The guided light is divided into two optical waveguides (arms), and after travelling in these two waveguides, they are recombined by a coupler into a single waveguide. If the interferometer is symmetric, there is no phase difference between the light that arrives in the second coupler and they combine constructively to produce maximum output. However, if a phase difference is introduced between the light guided in the two arms, the output is different, and is expressed by:

$$I_{output} = \frac{I_{input}}{2}(1 + \cos\phi) \qquad (5)$$

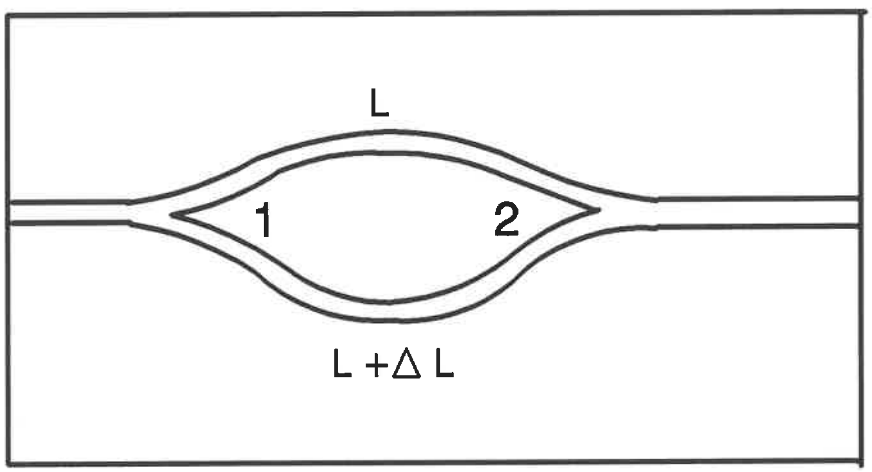

Figure 1.4 Schematic diagram of a Mach-Zehnder interferometer

where the angle ϕ is the phase difference between the light guided in the two arms of the interferometer. This effect can be employed to produce a number of practical devices such as pressure and refractive index sensors, and all-optical switches. In all of these devices a change in one arm is used to produce the phase difference.

In telecommunication and CATV subscriber networks, there is a need to wavelength division multi/demultiplexing of the two important wavelengths 1.30 and 1.55 μm . **Figure 3.1** in Chapter 3 depicts a Mach-Zehnder type wavelength division multi/demultiplexer (WDM) for 1.30 and 1.55 μm wavelengths. The light to be demultiplexed is split into the interferometer arms by a symmetric 3dB splitter. Light interferes in a four-port hybrid optical coupler, which consists of a symmetric Y-branch and an asymmetric adiabatic Y-branch. The symmetric part of this coupler combines the evenly split light into the local guided modes of the coupler junction. If the phase difference in the two interferometer arms is zero, all of the light is coupled to the local fundamental mode. With the phase difference of π, light is coupled to the higher order (antisymmetric) mode. With other values for the phase difference, optical power is divided to both modes according to this phase difference. The nonsymmetric branch of the coupler acts as a mode splitter: with proper adiabatic conditions the fundamental mode is coupled to the output waveguide with high effective index, the antisymmetric mode is coupled to the other waveguide. In the devices, where curves and straight waveguides are joined, 0.25 μm offsets are used to decrease the radiation loss at the joints due to shift of modefield in curves. In the joint bends with opposing directions, 0.5 μm offsets are used. In **Figure 1.5**, an optical micrograph shows such an offset. The 1.30 and 1.55 μm WDM is used in the investigations reported in Chapters 2, 3 and 4.

Erbium-doped fibre amplifiers have an increasingly important role in optical telecommunications. These amplifiers comprise various components, one of which is the wavelength division multiplexer (WDM) for injecting the light from pump laser into the doped fibre. The two important pump laser wavelengths are 0.98 and 1.48 μm. The integrated optics approach for WDM component is an interesting alternative (see **Figure 4.1** in Chapter 4). Integrated optics WDM devices can be hybridized with the doped fibre and laser diodes to form a compact amplifier module. Other guide-wave elements such as 1/N splitter can be integrated on the same substrate.

A 1.48/1.55 μm WDM was successfully produced to multiplex 1.48 μm and 1.55 μm wavelengths. It was designed similar to the 1.3/1.55 μm WDM described above. The details of fabrication and testing are reported in Chapters 3 and 4.

This project has contributed to about 10 conference and journal publications. A list of these publications is given below.

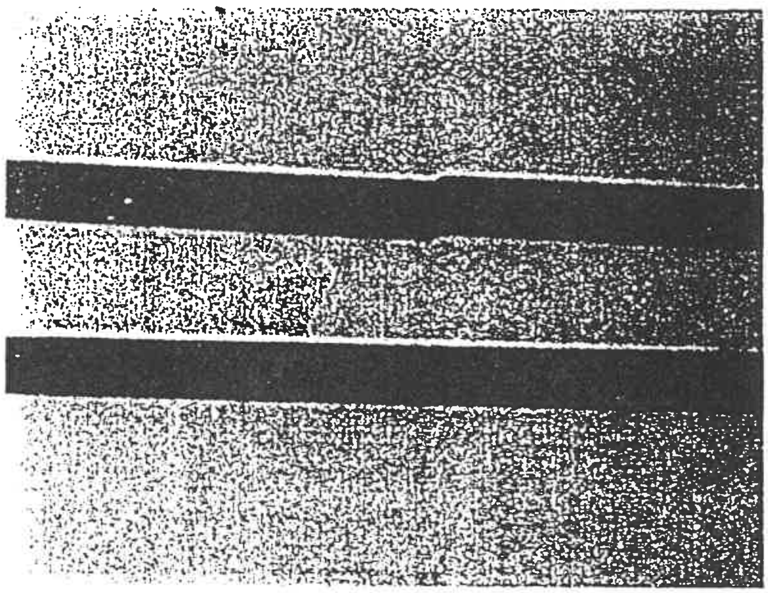

Figure 1.5 Microscope photograph of the offset

Magnification: 100 X

1. "Effect of thermal post-annealing on spectral transmission of ion-exchanged glass waveguide Mach-Zehnder interferometer multi/demultiplexers", *Integrated Optics*, Lindau, Germany, 1994.

2. "Glass integrated optical circuit for 1.30/1.55 micrometer optical communication system", *Integrated Optics*, Lindau, Germany, 1994.

3. "Modified double ion-exchange method for the fabrication of phase gratings in glass waveguides", *Integrated Optics,* Lindau, Germany,1994.

4. "Ion-exchanged glass waveguide Mach-Zehnder interferometer for wavelength multi/demultiplexer and the effect of thermal post-annealing on special transmission". *JEOS-Pure and Applied Optics,* submitted.

5. "Fabrication, optical characterization and femtosecond pulse propagation in a semiconductor quantum dot waveguide", to be published.

6. "Glass integrated optics circuit for 1.48/1.55 μm WDM, 1.30/1.55 μm WDM and 1/8 splitting", *Appl. Opt.*, to appear in June, 1994 issue.

7. "Low loss integration of 1.30/1.55 μm wavelength multiplexer and 1/8 splitter in glass waveguides", *OSA/ILS '93,* Toronto, 1993.

8. "1.30/1.55 μm and 1.48/1.55 μm wavelength multiplexers/demultiplexers", *OSA/ILS '93,* Toronto, 1993.

9. "Passive and active computer-generated waveguide holograms", *OSA/ILS '93,* Toronto, 1993.

10. "Integrated 1.30/1.55 μm wavelength multiplexer and 1/8 splitter by ion exchange in glass", *Electron. Lett.*, No.12, pp.1064-1066,1993.

In this thesis, three journal publications concerning the integrated optics WDM and power splitters in glass are included.

In Chapter 2, *Integrated 1.30/1.55 μm wavelength multiplexer and 1/8 splitter by ion exchange in glass* is demonstrated. This work was published in Electronics Letters (June 10th, 1993 Vol.29 No.12 pp.1064-1065).

In Chapter 3, *Ion-exchanged glass waveguide Mach-Zehnder interferometers for wavelength multi/demultiplexing and the effect of thermal post-annealing on spectral transmission* is studied. This paper is submitted to JEOS-Pure and Applied

Optics.

In Chapter 4, *Glass integrated optics circuit for 1.48/1.55 μm and 1.30/1.55 μm wavelength division multiplexing, and 1/8 splitting* is described. This paper has been accepted for publication in Applied Optics, and it will appear in the June 1994 issue.

Finally, in Chapter 5, the summary of the thesis is given and future work is proposed.

1.7 References

[1]. Miller. S. E., "Integrated optics: an introduction", *Bell Sys. Tech. J.*, Vol. 48, pp. 2056-2068, 1969.

[2]. H. Nishihara, M. Haruna and T. Suhara, "Optical integrated circuits", Mcgraw-Hill, New York, 1989.

[3]. S. I. Najafi, "Introduction to Glass Integrated Optics", Artech House, Boston, 1992.

[4]. Izawa T. and H. Nakagome, "Silver ion-exchanged glass waveguides", *Appl. Phys. Lett.*, Vol. 21, pp. 584-586, 1972.

[5]. Walker R. G., C. D. W. Wilkinson and J. A. H. Wilkinson, "Integrated optical waveguiding structures made by silver ion-exchange in glass: 1. The propagation characteristics of strip ion-exchanged waveguides; a theoretical and experimental investigation", *Appl. Opt.*, Vol. 22, pp. 1923-1928, 1983.

[6]. J.Viljanen and M. Leppihalme, "Analysis of loss in ion-exchange glass waveguides", *Proc. 1st Eur. conf. Integrated Optics*, pp.18, 1981.

[7]. J. Albert, W. J. Wang and S. I. Najafi, "Optical damage threshold of ion-exchanged glass waveguides at 1.06 μm", *Conference on Integrated Optics Circuits,* Paper #4, Boston, 1991.

[8]. Ionex software, Optonex Ltd., Espoo, Finland.

[9]. Y. Cheng, W. Lin and Y. Fujii, "Local field analysis of bent graded-index planar waveguides", *J. Lightwave Tech.*, Vol. 8, pp. 1461-1469, 1990.

[10]. E. Kapon and R. N. Thurston, "Multichannel waveguide junctions for guide-wave optics", *Appl. Phys. Lett.*, Vol. 50, No. 24, pp. 1710-1712, 1987.

[11]. E. Okuda, I. Tanaka and T. Yamasaki, "Planar gradient-index glass waveguide and its applications to a 4-port branched circuits and star coupler", *Appl. Opt.*, Vol. 3, pp. 1745-1748, 1984.

[12]. G. V. Tteyz, "Silicon Mach-Zehnder waveguide interferometer operating at 1.30 μm", *Electron. Lett.*, Vol. 27, pp. 118-120, 1991.

[13]. N. A. Sanford, K. J. Malone, D. R. Larson and R. K. Hickemell, "Y-branch waveguide glass laser and

amplifier", *Opt. Lett.*, Vol. 16, pp. 1168-1170, 1991.

[14]. J. Saarinen, J. Huttunen, S. Honkanen, S. I. Najafi and J. Turunen, "Computer-generated waveguide holograms by double ion-exchange process in glass", *Electron. Lett.*, Vol. 28, No.9, pp. 876-878, 1992.

CHAPTER 2

published in the journal: *Electronics Letters*,
10th June 1993, Vol. 29, No. 12, pp. 1064-1066

INTEGRATED 1.3 μm/1.55 μm WAVELENGTH MULTIPLEXER AND 1/8 SPLITTER BY ION EXCHANGE IN GLASS

G. Zhang, S. Honkanen, S. I. Najafi and A. Tervonen

Photonics Group of Montreal, Ecole Polytechnique,

P. O. Box 6079, Station A, Montreal (Quebec) H3C 3A7, Canada

Abstract: Integration of a 1.3 μm/1.55 μm wavelength multiplexer and a 1/8 splitter in a single glass substrate is demonstrated by potassium and silver double-ion exchange. The device is composed of a nonsymmetric Mach-Zehnder interferometer for wavelength multiplexing and symmetrical Y-junctions for achromatic splitting. The facet-to-facet excess loss is less than 2.5 dB.

Indexing terms: Integrated optics, optical waveguides

2.1 Introduction

Optical fibres are emerging rapidly in telecommunication and CATV subscriber networks [1]. In these networks there is a need for high performance, inexpensive and reliable passive optical components, such as wavelength independent 1/N splitters and wavelength selective couplers for wavelength division multiplexing (WDM). Integrated optical components made by planar techniques are suitable for mass production and have a strong potential to meet the requirements of the subscriber networks. To fully exploit the benefits of integrated optics, several components should be integrated in a single substrate, which increases the reliability and reduces the costs for fibre attachment and packaging. However, the more complex device configurations increase the reproducibility requirements for fabrication processes, and device designs with more relaxed fabrication tolerances are needed.

In this letter, we demonstrate the integration of 1.30/1.55 μm wavelength multiplexer and a 1/8 splitter in a single glass substrate by a simple ion exchange process. The device, which can be applied in future WDM-subscriber networks, is shown schematically in **Figure 2.1.** It consists of a nonsymmetric Mach-Zehnder interferometer for wavelength multiplexing [2] and symmetrical Y-branches for achromatic splitting. The advantage of these waveguide structures

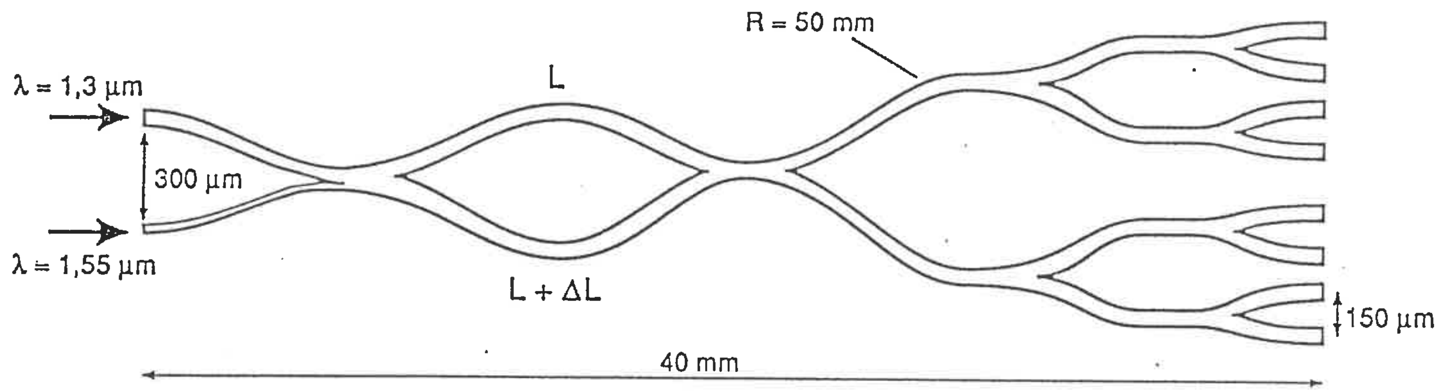

Figure 2.1 Schematic diagram of the integrated wavelength multiplexer and 1/N splitter

(compared with, for example, directional couplers) is the low sensitivity to fabrication conditions and optical polarisation.

2.2 Device Operation and Design

In our device, light at 1.55 μm wavelength and at 1.30 μm wavelength is coupled into the two separate inputs of the asymmetric adiabatic Y-branch of the wavelength multiplexer (see **Figure 2.1**). For proper adiabatic operation, mask opening widths of 2.5 and 5.5 μm and an angle of 3 mrad were chosen for the asymmetric Y-branch. In other parts of the device, 4 μm mask opening width is used. The light at 1.3 μm wavelength from the wider arm of the asymmetric Y-branch, which has higher effective index, is coupled to the symmetric mode of the asymmetric/symmetric Y-branch junction, and light at 1.55 μm wavelength from the narrower arm of the asymmetric Y-branch is coupled to the antisymmetric mode of the junction. At both wavelengths, light is then split evenly to the two arms of the Mach-Zehnder interferometer with a phase difference in the two arms of zero at 1.3 μm wavelength and π at 1.55 μm wavelength. At the output end of the Mach-Zehnder interferometer light is combined by a symmetrical Y-branch, and at both wavelengths, the phase difference of light from the two arms has to be zero in order to optimally couple light to the 1/8 splitter. This is achieved by a proper design of the optical path length difference between the two arms of the Mach-Zehnder interferometer. It was designed as 2.5 and 3 "guided wave wavelengths", respectively, at 1.55 and 1.3 μm "vacuum wavelengths". In the design, a model for optical propagation in silver ion-exchanged waveguides in Corning 0211 glass was used [3], and also the change in propagation constants and the shift of mode fields in curves were taken into account [4]. The designed geometrical path length difference in the nonsymmetric Mach-Zehnder interferometer is 2.565 μm and the bend radius used is 50 mm.

For the achromatic 1/8 splitting, symmetrical Y-branches are used. They are formed by S-bends with 50 mm radii of curvature. Where curves and straight waveguides are joined in the device, 0.25 μm offsets are used to decrease the radiation loss at the joints due to shift of mode field in curves. In joints of bends of opposing directions 0.5 μm offsets are used. The total active length of the device is 37 mm, with 300 μm separation between the two input waveguides and 150 μm between the output waveguides.

2.3 Fabrication

The integrated wavelength multiplexer and 1/8 splitter was fabricated by potassium and silver double-ion exchange process [5], although the device was designed for silver ion exchange. The use of double-ion exchange process was possible, because the waveguide structures used are rather insensitive to the fabrication conditions. The double-ion exchange was chosen, because low loss waveguides can be achieved even by using aluminium as a mask during the silver ion exchange step [6, 7]. A conventional photolithography was used to define the mask openings in an aluminium film on a 0.5 mm thick Corning 0211 glass substrate. The sample was immersed in a potassium nitrate melt at 400^0C for 165 min. A silver ion exchange was then performed for 210 min in a silver nitrate melt at 300^0C. After the ion exchange process, the aluminium film was removed, and the substrate was polished to a 40 mm long chip.

2.4 Measurements

For the device characterization a single-mode fibre was used to launch light separately from 1.3 and 1.55 μm laser diodes into the respective input waveguide. First the output facet was viewed with a microscope objective and an infra-red camera. The near-field photograph of the output waveguides of the device is shown in **Figure 2.2a** for 1.3 μm wavelength and in **Figure 2.2b** for 1.55 μm wavelength. The fibre-device insertion loss measurements were performed by collecting the light from the output ports with a microscope objective to a photodetector. The measured insertion loss (including the input fibre-chip coupling and the eight-way splitting) for each output port is shown in **Figure 2.3a** for 1.3 μm wavelength

(a)

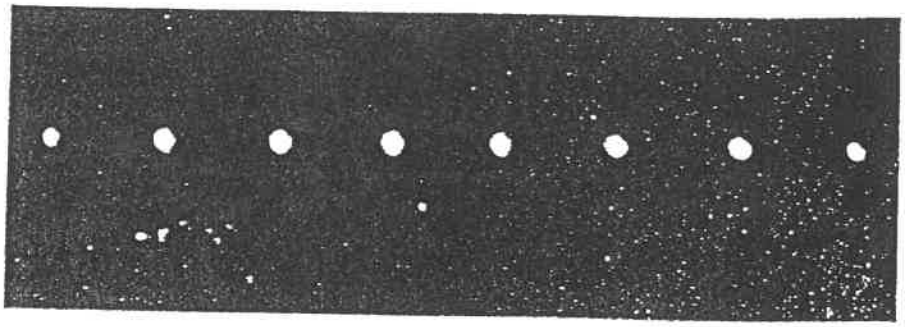

1.30 μm

(b)

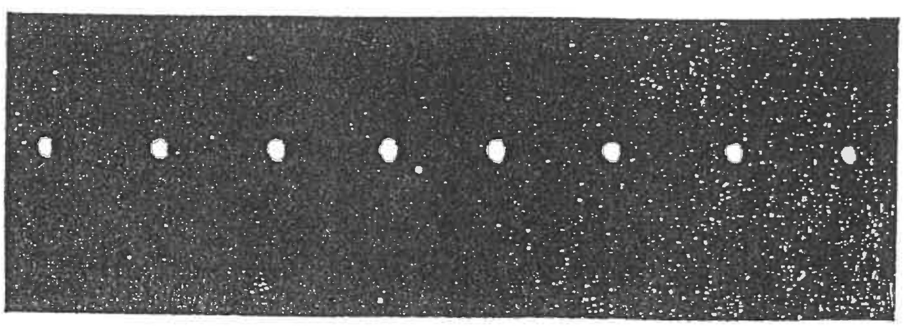

1.55 μm

Figure 2.2 Nearfield photograph of output waveguides of the device (a) at 1.30 μm and (b) at 1.55 μm

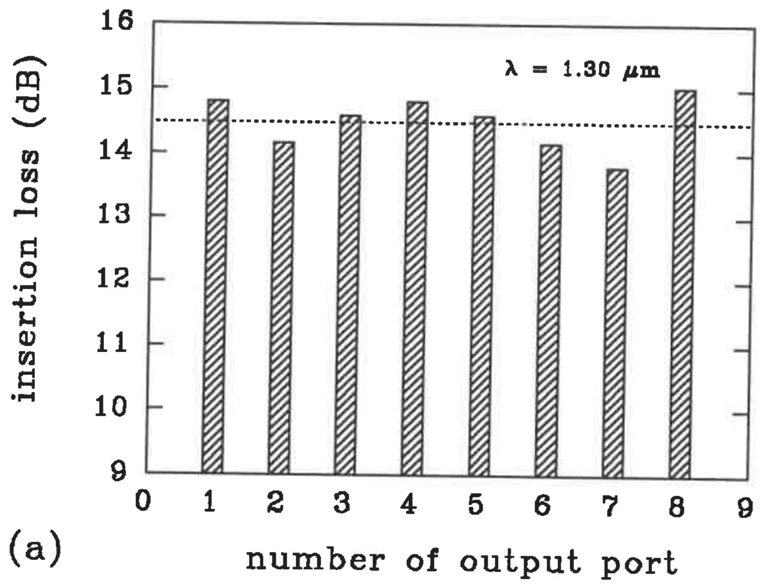

(a)

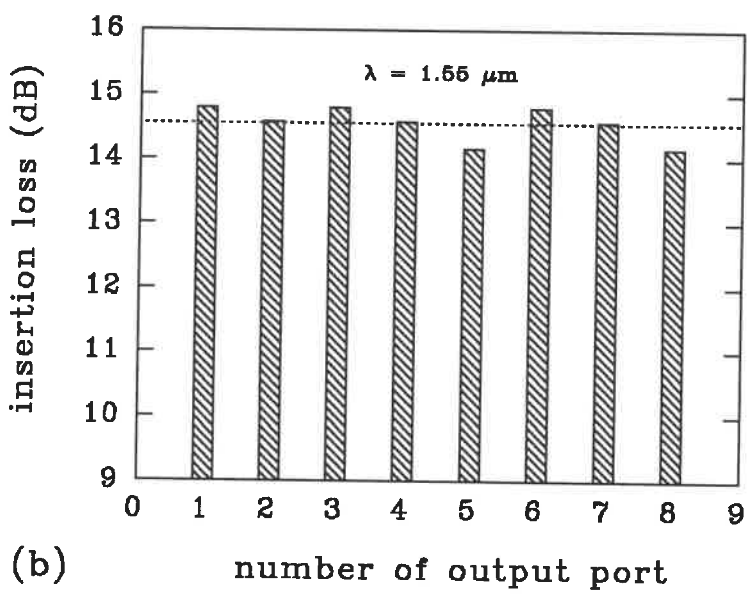

(b)

Figure 2.3 Measured fiber–chip insertion loss of the integrated 1.30/1.55 μm wavelength multiplexer and 1/8 splitter (a) at 1.30 μm (b) at 1.55 μm

and in **Figure 2.3b** for 1.55 μm wavelength. At 1.3 μm wavelength, the mean insertion loss is 14.49 dB with a standard deviation of 0.39 dB and a maximum deviation of 0.70 dB. At 1.55 μm wavelength the mean insertion loss is 14.55 dB with a standard deviation of 0.25 dB and a maximum deviation of 0.40 dB. From separate measurements at 1.3 μm wavelength of straight waveguides fabricated with similar parameters, we know that the coupling loss of these small mode size double-ion-exchanged waveguides with a fibre is over 3 dB (note that the fibre-chip coupling loss can be considerably reduced, for example, by thermally tapering the input and output waveguides [8]), and the waveguide loss is 0.25 dB/cm. Therefore, the facet-to-facet excess loss, at both wavelengths, is less than 2.5 dB, of which 1 dB is waveguide loss and only 1.5 dB is due to the device configuration.

2.5 Conclusion

We have fabricated an integrated 1.3 μm/1.55 μm wavelength multiplexer and a 1/8 splitter in a single glass substrate by a simple double-ion exchange process. The measured facet-to facet excess loss in the 40 mm long chip is less than 2.5 dB, although we used aluminium as a masking material for ion exchange and an inexpensive multipurpose glass as a substrate.

2.6 Acknowledgement

This work is funded in part by a university-industry co-operative research grant from National Sciences and Engineering Research Council (NSERC) of Canada and Bell Northern Research (BNR).

2.7 References

[1]. D. B. Keck, A. J. Morrow, D. A. Nolan, and D. A. Thompson, "Passive components in the subscriber loop", *J. Lightwave Technol.*, LT-7, pp. 1623-1633, 1989.

[2]. A. Tervonen, P. Pöyhönen, S. Honkanen, and M. Tahkokorpi, "A guided-wave Mach-Zehnder interferometer structure for wavelength multiplexing", *IEEE Photonics Technol. Lett.*, pp. 516-518, 1991.

[3]. A. Tervonen, P. Pöyhönen, S. Honkanen, M. Tahkokorpi, and S. Tammela, "Examination of two-step fabrication methods for single-mode fibre compatible ion-exchanged glass waveguides", *Appl. Opt.*, pp. 338-343, 1991.

[4]. Y. Cheng, W. Lin, and Y. Fujii, "Local field analysis of bent graded-index planar waveguides", *J. Lightwave Technol.*, LT8, pp. 1461-1469, 1990.

[5]. S. I. Najafi, "Waveguides and devices", in Najafi (Ed.): "Introduction to glass integrated optics" (Artech House, Boston, 1992), Chap. 6.

[6]. W. J. Wang, S. Honkanen, S. I. Najafi, and A. Tervonen, "New integrated optical ring resonator in glass",

Electron. Lett., Vol. 28, pp. 1967-1968, 1992.

[7]. H. Helmers, O. G. Helleso, P. Benech, and R. Rimet, "Single mode potassium and silver ion-exchanged glass waveguides with low losses and high index increase", *Appl. Phys. Lett.*, pp. 2759-2760, 1992.

[8]. A. Mahapatra, and J. M. Connors, "Thermal tapering of ion-exchanged channel guides in glass", *Opt. Lett.*, 3, pp.169-171, 1988.

CHAPTER 3

Accepted for publication by the journal: *JEOS-Pure and Applied Optics*.

ION-EXCHANGED GLASS WAVEGUIDE MACH-ZEHNDER INTERFEROMETERS FOR WAVELENGTH MULTI/DEMULTIPLEXING AND THE EFFECT OF THERMAL POST-ANNEALING ON SPECTRAL TRANSMISSION

Guangwen Zhang, Seppo Honkanen, Ari Tervonen, Pekka Katila and S. Iraj Najafi

Photonics Group of Montreal, École Polytechnique
P.O. Box 6079, Station A, Montreal (Quebec) H3C 3A7, Canada

***Abstract*:** Nonsymmetric three-port integrated optical Mach-Zehnder interferometer configuration is employed to make 1.30/1.55 μm and 1.48/ 1.55 μm wavelength multiplexers and demultiplexers. The devices are produced by potassium-silver double-ion exchange process. The effect of thermal post-annealing on spectral behaviour of the fabricated devices is investigated. It is observed that the 1.3/1.55 μm device is not sensitive to post-annealing while the transmission spectrum of the 1.48/1.55 μm changes after post-annealing. The losses and extinction ratios of the fabricated devices are also determined.

Indexing terms: Integrated optics, optical waveguides

3.1 Introduction

Passive integrated optical devices, such as power dividers and wavelength multi/demultiplexers (WDM), made by ion exchange techniques in glass [1] have considerable potential use in fibre-optic communication systems [2]. In future WDM-systems there is need for dual WDM-components for several combinations of two wavelengths. They can be used to multi/demultiplex the important transmission wavelengths 1.30 μm and 1.55 μm, and to multiplex the signal and pump wavelengths (e.g. 1.48 μm and 1.55 μm) of an optical fibre amplifier.

A typical choice for a dual WDM-component has been a symmetric directional coupler [3-5]. It is a simple structure and has the advantage of small size and low optical losses. However, the spectral transmission characteristics of symmetric directional couplers are very sensitive to fabrication conditions and it seems difficult to reproducibly achieve devices with desired centre wavelengths and low crosstalk. Another choice for a dual WDM-component is a nonsymmetric guided-wave Mach-Zehnder interferometer having no directional coupler splitters [5, 6]. It is a more complex device, but offers the advantage of high tolerances for fabrication process deviations, which is of crucial importance in passive integrated optics.

In this paper, we present an experimental study of spectral transmission characteristics of three-port Mach-Zehnder interferometer multi/demultiplexers. The components are designed for wavelength combinations 1.30/1.55 μm and 1.48/1.55 μm, and they are fabricated by potassium and silver double-ion exchange process [7]. Their sensitivity to fabrication conditions and the possibility to tune their characteristics afterwards are studied by thermally post-annealing the components.

3.2 Mach-Zehnder Interferometer WDM-Devices

A. Description

A three-port nonsymmetric Mach-Zehnder interferometer is sketched schematically in **Figure 3.1**. It is composed of an adiabatic asymmetric Y-branch (#3 in **Figure 3.1**) and two symmetric Y-branches (#1 and #2 in **Figure 3.1**), which are connected to each other by two waveguides having different lengths (L and L + ΔL). This path length difference in the actual interferometer part of the device determines its wavelength-dependent operation. When the device is used as a demultiplexer, light is coupled to the single input waveguide (i.e. from the left in **Figure 3.1**). gwght is then split equally by the first symmetric Y-branch into the two interferometer arms and combined by the second symmetric Y-branch. Due to the path length difference, the phase

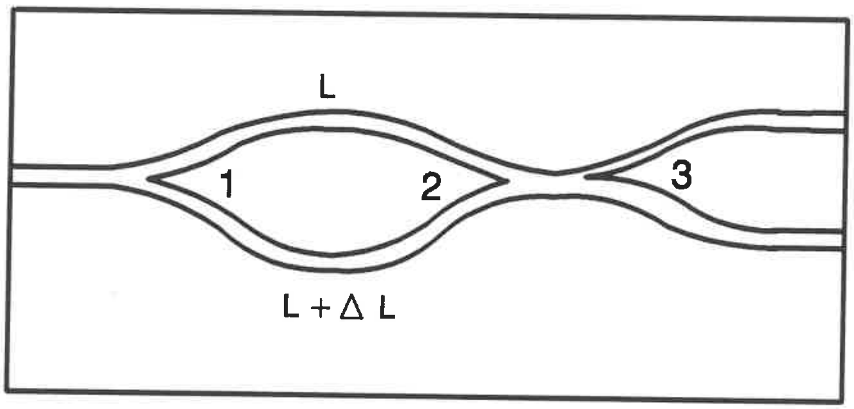

Figure 3.1 Schematic diagram of three-port nonsymmetric Mach-Zehnder interferometer

difference between light from the two interferometer arms depends on wavelength. For proper operation, the phase differences have to be zero and π at the two wavelengths to be demultiplexed. At the symmetric/asymmetric Y-branch junction, light with zero phase difference excites the fundamental mode, and it is coupled to the wider arm of the asymmetric adiabatic Y-branch. Light with phase difference of π excites the antisymmetric mode of the junction and is coupled to the narrower arm of the asymmetric adiabatic Y-branch [5].

Since the behaviour of the Y-branches depends very little on the wavelength, the spectral transmission properties of the WDM-device are determined only by the optical path length difference between the two interferometer arms. As described above, the path length difference is achieved by using different lengths of curved waveguides in the interferometer arms. However, in designing the device, also the shift of modefields [8] in curved waveguides has to be taken into account. This shift depends upon fabrication conditions, and it controls the spectral transmission properties of the WDM-device. For example, by post-annealing the ion-exchanged device the modefield shifts outwards in the bends, and the path length difference increases. The dependence decreases with decreasing the path length difference and increasing the bend radius.

B. Design

In order to study the device sensitivity to fabrication conditions (and the possibility of tuning by post-annealing), we designed two WDM-devices: a) the first one (1.30/1.55 μm) having a short path length difference and a relatively large bend radius, and b) the second one (1.48/1.55 μm) with longer path length difference and smaller bend radius. The waveguides were designed for silver ion exchange in Corning 0211 glass [9], and the shift of modefields in curves was also taken into account [10]. The designed geometrical path length difference in the 1.30/1.55 μm WDM-device is 2.565 μm, and the bend radius is 50 mm. In the 1.48/1.55 μm WDM-device these values are 10.75 μm and 30 mm, respectively. Both devices were designed to couple 1.55 μm wavelength to the narrower arm of the asymmetric Y-branch. The mask opening widths in the asymmetric Y-branch are 2.5 μm and 5.5 μm and the branching angle is 3 mrad. In other parts of the devices 4 μm mask opening width is used.

3.3 Fabrication

The WDM-devices were fabricated by potassium and silver double-ion exchange process, although they were designed for silver ion exchange. The double-ion exchange was chosen, because low loss waveguides could be obtained easily even with aluminum as a masking material. The formation of loss producing silver particles during silver ion exchange was reduced considerably due to the first step potassium ion exchange [11]. At present time, the double-ion exchange process is not understood well enough, so it is not possible to design the waveguides for this process. However, the behaviour of the studied Mach-Zehnder interferometers is so insensitive to fabrication conditions that double-ion exchange could be employed.

A conventional photolithography process was used to define mask openings in a 1000 Å thick aluminum film on Corning 0211 glass substrates. First, the samples were immersed in a potassium nitrate molten bath at 400°C. Then, a silver ion exchange was performed in a silver nitrate molten bath at 300°C. After ion exchange processes, the aluminum films were removed and the two end faces of the samples were polished for optical measurements. The thermal post-annealing was performed by heating the samples in a furnace at 300°C. Ion exchange and post-annealing times are provided in **Table 3.1**.

3.4 Measurements and Results

Figure 3.2 depicts schematically the setup used for characterization of the fabricated devices. A white light source, a He-Ne laser, and two laser diodes around 1.3 μm and

Table 3.1 Device fabrication parameters. Potassium and silver ion exchanges were carried out at 400°C and 300°C, respectively.

Device	**Ion exchange time (min)**		**Post-annealing time (min)**
	Potassium ion	Silver ion	300°C
1.30/1.55 μm WDM	165	180	120
1.48/1.55 μm WDM	165	210	68

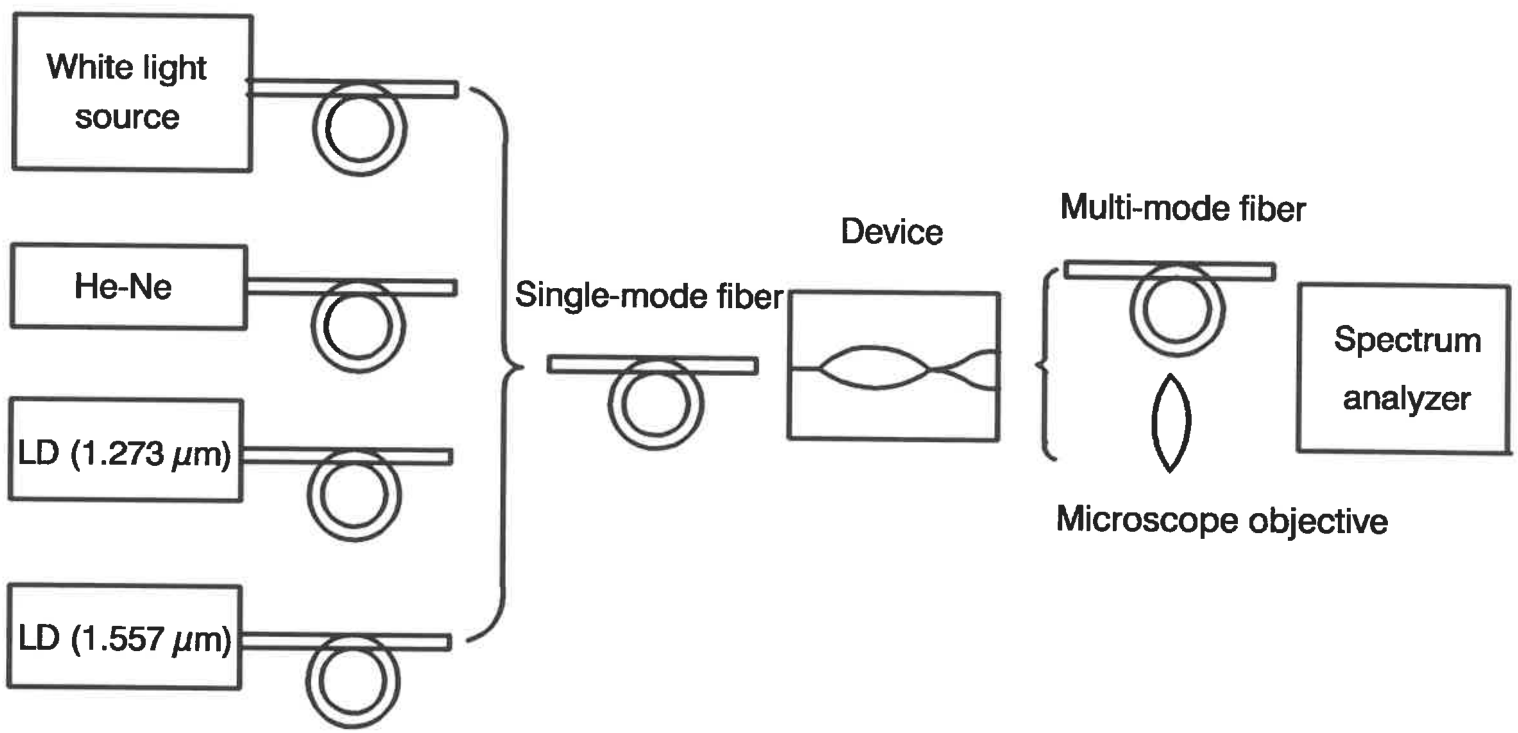

Figure 3.2 Measurement set-up

1.55 μm wavelengths were used in the characterization. The wavelengths of the laser diodes were 1.273 μm and 1.557 μm, which were utilized to measure loss and cross-talk. He-Ne laser was employed simply for the initial alignment. White light source was used for transmission spectrum measurements. The 1.273 μm laser diode was also used to make sure that the fundamental mode of the input waveguide of the device was excited by the fibre prior to transmission spectrum measurements. A single-mode optical fibre was used to couple light into the devices and a multimode fibre was utilized to collect the output light from the device. The output light was then measured by a spectrum analyzer.

The transmission spectra of both 1.30/1.55 μm and 1.48/1.55 μm devices were measured as demultiplexers. Non-polarized light was used in the measurements. **Figure 3.3** summarizes the measurement results of the 1.30/1.55 μm demultiplexer before and after post-annealing. **Figure 3.4** shows the results for 1.48/1.55 μm demultiplexer.

In fibre-device insertion loss measurements, the devices were employed as demultiplexers. Light from 1.273 μm and 1.557 μm laser diodes were coupled into the common waveguide of the demultiplexer and were collected from the output ports to a photodetector using a microscope objective. The transmission of the microscope objective was measured separately. Here, the extinction ratio in the device, when used as a demultiplexer was also measured. The measured

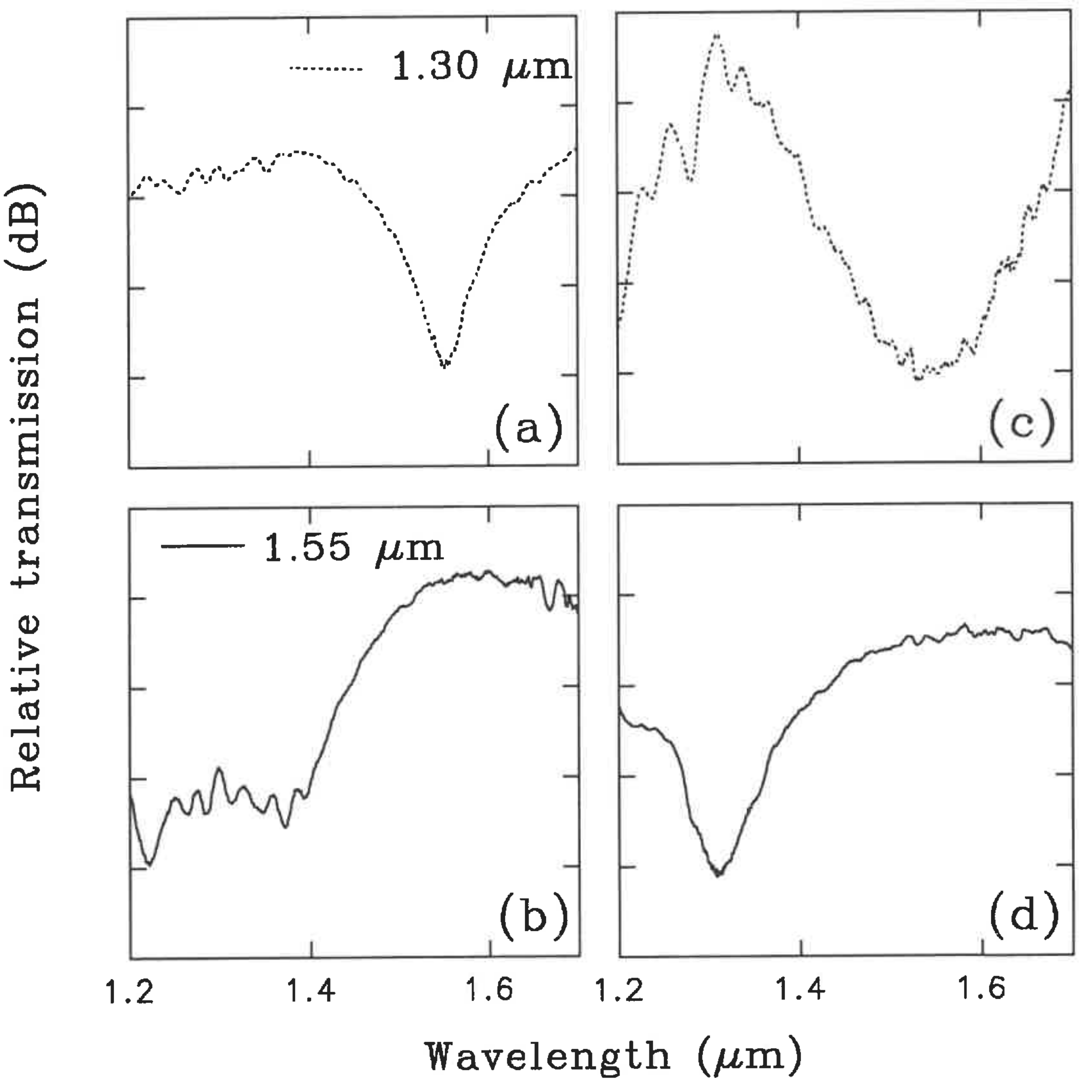

Figure 3.3 Measured spectral transmission of 1.30/1.55 μm wavelength demultiplexer

a) and b) before post-annealing
c) and d) after post-annealing

Dotted and solid curves are outputs from wide and narrow arms, respectively.

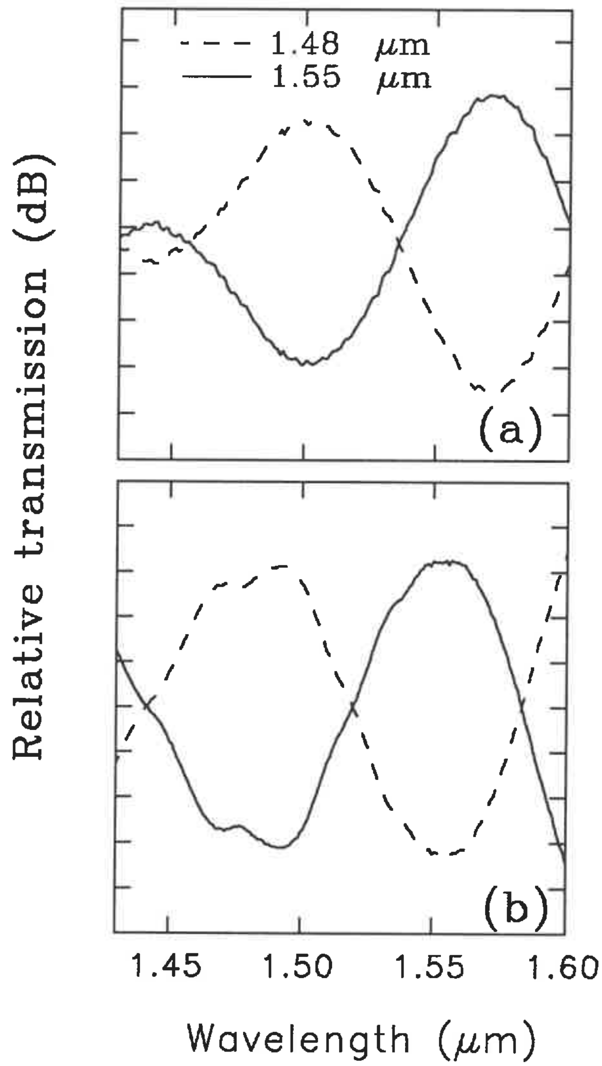

Figure 3.4. Measured spectral transmission of 1.48/1.55 μm wavelength multiplexer

a) before post−annealing

b) after post−annealing

Dashed and solid curves are outputs from wide and narrow arms, respectively.

losses and extinction ratio measurement results are summarized in **Table 3.2**. The extinction ratio is defined as the ratio of the output from two ports at the two wavelengths. For the 1.48/1.55 μm demultiplexer, the extinction ratio was measured only at 1.55 μm wavelength because 1.48 μm laser source was not available. It is worth noting that the prime application of this device is wavelength multiplexing, and the high extinction ratio is not so important. The losses are determined as explained elsewhere [11]. Our goal in this work was not to achieve low fibre to waveguide coupling loss. This loss can of course be reduced significantly [12].

3.5 Discussion and Conclusion

We have employed potassium and silver double ion-exchange process to make 1.30/1.55 μm and 1.48/1.55 μm three-port integrated optical Mach-Zehnder interferometers in glass for multi/demultiplexer applications. A detailed optical characterization was carried out and, in particular, the effect of post-annealing on the device behaviour was investigated.

The overall spectral characteristics of the 1.30/1.55 μm device are not sensitive to post-annealing. The centre wavelength of "stop band" remains the same. Since the waveguides are multimode around 1.30 μm wavelength, some oscillations in the transmission spectra occur. Post-

Table 3.2 Extinction ratio of the fabricated WDMs. The facet-to-facet excess loss at the three operation wavelengths was around 1 dB. The fibre to waveguide coupling loss was about 3.5 dB per facet.

Device	**EXTINCTION RATIO (dB)**			
	Before annealing		After annealing	
	λ=1.273 μm	λ=1.557 μm	λ=1.273 μm	λ=1.557 μm
1.30/1.55 μm WDM	7.6	17.0	13.0	12.0
1.48/1.55 μm WDM	-	6.1	-	19.0

annealing improves the device behaviour and increases the extinction ratio at this wavelength because more light from the fibre is coupled in the fundamental mode (whose mode profile has become larger). The obtained extinction ratio is relatively high because the measurement wavelength is not very close to the centre wavelength of the "stop band". At 1.55 μm, the extinction ratio decreases because the waveguide becomes two modes after long post-annealing. To eliminate completely this behaviour wide single mode region waveguides should be made. This can be achieved, for example, by burying the waveguides.

By contrast, the spectral characteristics of the 1.48/1.55 μm device are sensitive to post-annealing. This was expected because of the longer pathlength difference between the two arms of the interferometer and the smaller bend radii. This effect can be employed positively in the production of the device because a high accuracy is usually needed when the wavelength spacing is very small. Post-annealing can be used for fine-tuning of the optical characteristics of these devices after fabrication is completed.

The measured facet-to-facet excess loss in the fabricated devices is less than 1.0 dB although we used aluminum as a masking material for ion exchange and an inexpensive multipurpose glass as a substrate. The fabricated passive integrated optical devices can be employed in connection with an Er-doped fibre in future WDM subscriber networks, in which amplification at 1.55 μm is needed. A similar device can be made to amplify the 1.30 μm light (0.807 μm/1.3 μm if Nd-doped fibre is used). The 1.30/1.55 μm device can be employed to multiplex the two amplified signals. It can also be used to demultiplex these two signals as needed.

3.6 Acknowledgment

This work was funded in part by a University-Industry research grant from Natural Sciences and Engineering Research Council (NSERC) of Canada and Bell-Northern Research (BNR).

3.7 References

[1] S.I. Najafi, "Introduction to Glass Integrated Optics", Artech House, Boston, 1992.

[2]. D.B. Keck, A.J. Morrow, D.A. Nolan, D.A. Thompson, *J. Light-wave Technol*, pp. 1623-1633, 1989.

[3]. A.H. Reichelt, P.C. Clemens and H.F. Mahlein, *Proc. SPIE 1128*, pp. 165-168, 1989.

[4]. C. Nissim, A. Beguin, P. Laborde, C. Lerminaux and M. McCourt, *Proc. EFOC/LAN 90*, 27-29 June 1990, Munich, IGI Europe 1990, pp. 114-116.

[5]. A. Tervonen, S. Honkanen and S.I. Najafi, "Analysis of symmetric directional couplers and asymmetric Mach-Zehnder interferometers as 1.30/1.55 μm dual wavelength demultiplexers/ multiplexers", *Optical Eng.*, Vol. 32, pp. 2083-2091, 1993.

[6]. A. Tervonen, P. Poyhonen, S. Honkanen and M. Tahkokorpi, *IEEE Photon. Technol. Lett.*, pp. 516-518, 1991.

[7]. M.J. Li, S. Honkanen, R. Leonelli, J. Albert and S.I. Najafi, *Appl. Phys. Lett.*, pp. 2607-2609, 1991.

[8]. W.J. Wang, S. Honkanen, S.I. Najafi and A. Tervonen, *Electron. Lett.* Vol. 28, pp. 1967-1968, 1992.

[9]. A. Tervonen, P. Poyhonen, S. Honkanen, M. Tahkokorpi and S. Tammela, *Appl. Opt.* Vol. 30, pp. 338-343, 1991.

[10]. Y. Cheng, W. Lin and Y. Fujii, *J. Lightwave Technol.* Vol. 8, pp. 1461-1469, 1990.

[11]. W. J. Wang, S. Honkanen, S.I. Najafi and A. Tervonen, *J. Appl. Phys.*, pp. 1529-1533, 1993.

[12]. S. I. Najafi, "Critical Review Conference on Integrated Optics and Optoelectronics", Jan. 1993, invited paper, *SPIE Proceeding* #CR45, pp. 358-368, 1993

CHAPTER 4

To be published in June 1994 issue in the journal: *Applied Optics*.

GLASS INTEGRATED OPTICS CIRCUIT FOR 1.48/1.55 μm WDM, 1.30/1.55 μm WDM AND 1/8 SPLITTING

G. Zhang, S. Honkanen, S. I. Najafi and A. Tervonen

Photonics Group of Montreal, Ecole Polytechnique,
P. O. Box 6079, Succ. A, Montreal (Quebec) H3C 3A7, Canada

Abstract: We demonstrate the integration, in a single glass substrate, of a 1.48/1.55 μm wavelength multiplexer, and a 1.30/1.55 μm wavelength multiplexer followed by a 1/8 splitter by potassium and silver double-ion exchange. The wavelength multiplexers are based on nonsymmetric three-port Mach-Zehnder interferometers, and symmetrical Y-junctions are used for achromatic splitting. The facet-to-facet excess loss is less than 2.5 dB in all devices. The device can be used, in connection with an Er-doped fibre, in future wavelength division multiplexing subscriber networks, in which amplification is needed at 1.55 μm wavelength.

Indexing terms: Integrated optics, optical waveguides

4.1 Introduction

Optical fibres are emerging rapidly in telecommunication and CATV subscriber networks [1]. In these networks high performance passive optical components such as wavelength independent 1/N power splitters and wavelength selective couplers for wavelength division multiplexing (WDM) are needed. The successive splitting in the subscriber network causes considerable decrease in optical power, and it may be necessary to compensate the power decrease by adding amplifiers in the network. This can be done at the 1.55 μm wavelength by utilizing Er-doped waveguides (i.e. fibres or planar waveguides). Therefore, also wavelength multiplexers to combine the pump (e.g. 1.48 μm) and signal wavelength (1.55 μm) in the Er-doped waveguide are needed.

Integrated optical components made by planar techniques are suitable for mass production and have a strong potential to meet the requirements of the subscriber networks. To fully utilize the benefits of integrated optics several components should be integrated in a single substrate, which increases the reliability and reduces the costs for fibre attachment and packaging. Planar glass waveguide amplifiers are studied extensively in several laboratories, and the aim is, in fact, to integrate the amplifiers with passive wavelength multiplexers and 1/N splitters in a single substrate. However, the characteristics of the planar waveguide amplifiers are far from those of fibre amplifiers, and even the integration of different passive devices in a single substrate is not simple due to demanding device designs with relaxed fabrication tolerances. Therefore, it may be a better approach to use an external Er-doped fibre in connection with a passive integrated optical circuit. This approach complicates the fibre pigtailing only slightly, since several fibres are to be coupled to the glass waveguide circuit.

In this paper we demonstrate the integration of a 1.48/1.55 μm wavelength multiplexer and a 1.30/1.55 μm wavelength multiplexer followed by a 1/8 splitter in a single glass substrate, fabricated by a simple ion exchange process. This integrated optics circuit, in connection with an Er-doped fibre (see **Figure 4.1**), may be applied in future WDM subscriber networks. The 1.48/1.55 μm wavelength multiplexer is used to combine pump and signal in an Er-doped fibre amplifier, whose output is then connected to the 1.55 μm input of the 1.30/1.55 μm wavelength multiplexer, which is followed by the 1/N splitter. The wavelength multiplexers are composed of an adiabatic asymmetric Y-branch and a nonsymmetric Mach-Zehnder interferometer [2], and symmetrical Y-branches are used for achromatic splitting. The advantage of these wave-guide structures (compared to, for example, directional couplers) is the low sensitivity to fabrication conditions [3] and optical polarization.

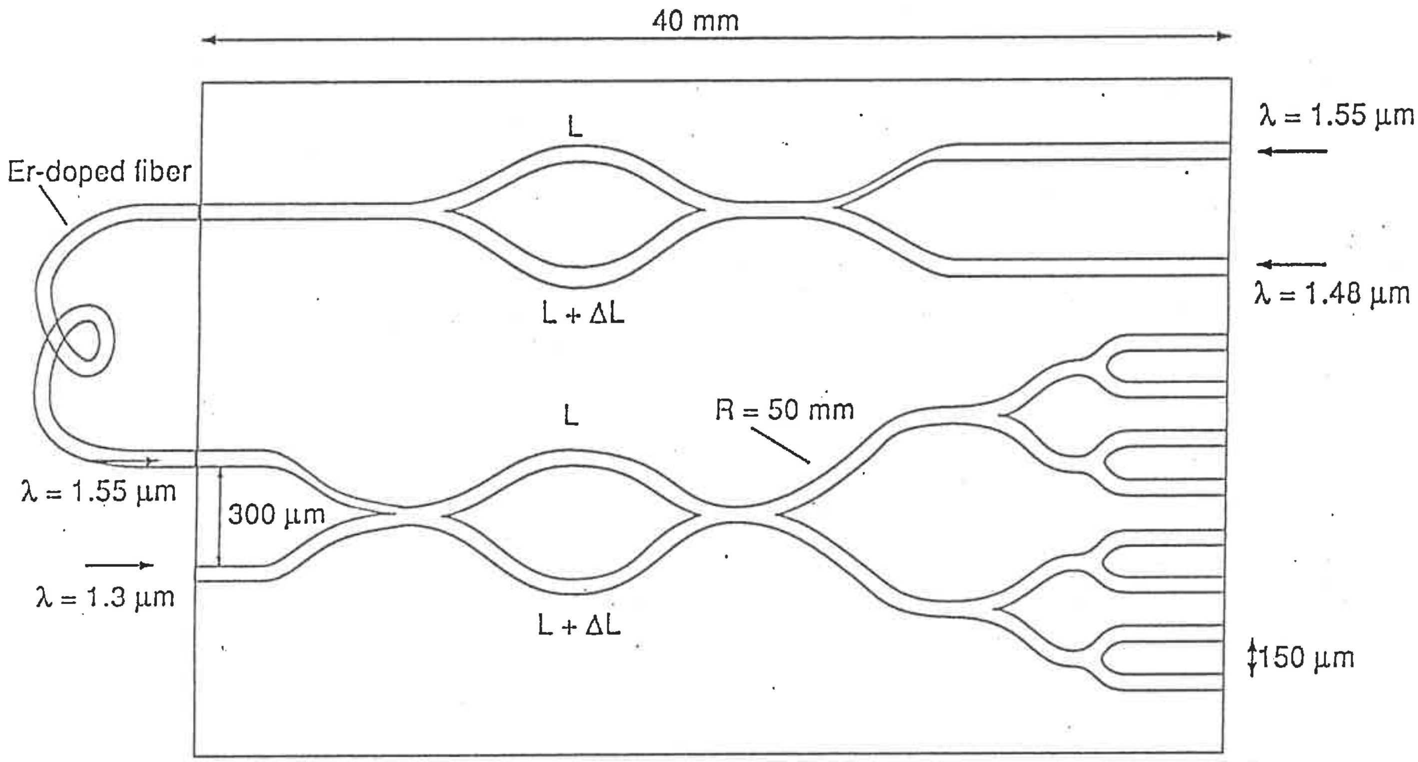

Figure 4.1 **Schematic diagram of the studied integrated optical circuit in connection with an Er-doped fiber**

4.2 Device Operation and Design

The pump at 1.48 μm wavelength and signal at 1.55 μm wavelength are coupled in the two separate inputs of the asymmetric adiabatic Y-branch of the 1.48/1.55 μm wavelength multiplexer (see **Figure 4.1**). For proper adiabatic operation, mask opening widths of 2.5 μm and 5.5 μm and an angle of 3 mrad were chosen for the asymmetric Y-branch. In other parts of the device 4 μm mask opening width is used. The light at 1.48 μm wavelength from the wider arm of the asymmetric Y-branch, which has higher effective index, is coupled to the symmetric mode of the asymmetric/symmetric Y-branch junction, and light at 1.55 μm wavelength from the narrower arm of the asymmetric Y-branch is coupled to the antisymmetric mode of the junction. At both wavelengths light is then split evenly to the two arms of the Mach-Zehnder interferometer with a phase difference in the two arms of zero at 1.48 μm wavelength and π at 1.55 μm wavelength. At the output end of the Mach-Zehnder interferometer light is combined by a symmetrical Y-branch, and at both wavelengths the phase difference of light from the two arms has to be zero in order to optimally couple light to the WDM output and to the Er-doped fibre. This is achieved by a proper design of the optical path length difference between the two arms of the Mach-Zehnder interferometer. It was designed as 10½ and 11 "guided wave wavelengths" respectively at 1.55 μm and 1.48 μm "vacuum wavelengths". In the design, a model for optical propagation in silver ion-exchanged waveguides in Corning 0211 glass was used [4], and also the change in propagation constants and the shift of modefields in curves [5] were taken into account. The designed geometrical path length difference in the nonsymmetric Mach-Zehnder interferometer is 10.75 μm and the bend radius used is 30 mm. With the calculated shift of the modefields in the curves, also lateral offsets could be designed for bend joints in order to decrease radiation losses. Where curves and straight waveguides are joined, this offset s=0.7 μm. For joints of bends in opposing directions, the offset is twice this. Since the path length difference in the interferometer is rather long and the bend radius rather small, the behaviour of the 1.48/1.55 μm multiplexer can be tuned by post annealing [6]. The post annealing decreases the mode confinement, which increases the shift of modefields in bends. This, in turn, increases the optical path length difference.

The 1.30/1.55 μm wavelength multiplexer was designed similarly as the 1.48/1.55 μm wavelength multiplexer. Here, the designed geometrical path length difference is only 2.565 μm corresponding to 2½ and 3 "guided wave wavelengths" respectively at 1.55 μm and 1.30 μm "vacuum wavelengths". The bend radius used is 50 mm and the offset in joints of curved and straight waveguides is s=0.25 μm. Due to the much shorter path length difference and larger bend radius the 1.30/1.55 μm wavelength multiplexer is very insensitive to fabrication parameters and its behaviour can be tuned only slightly by post annealing [6].

For the achromatic 1/8 splitting symmetrical Y-branches are used. They are formed by S-bends with 50 mm radii of curvature. Again, where curves and straight waveguides are joined, 0.25 μm offsets are used, and in joints of bends of opposing directions 0.5 μm offsets are used. The total active length of the device is 37 mm, with 300 μm separation between the input waveguides of the wavelength multiplexers and 150 μm between the 8 output waveguides.

4.3 Fabrication

The device was fabricated by potassium and silver double-ion exchange process [7], although the device was designed for silver ion exchange. The use of double-ion exchange process was possible, because the waveguide structures used are rather insensitive to the fabrication conditions. The double-ion exchange was chosen, because low loss waveguides can be achieved even by using aluminium as a mask during the silver ion exchange step [8]. A conventional photolithography was used to define the mask openings in an aluminum film on a 0.5 mm thick Corning 0211 glass substrate. The sample was immersed in a potassium nitrate melt at 400 °C for 165 min. Then a silver ion exchange was performed for 210 min in a silver nitrate melt at 300 °C. After the ion exchange process, the aluminum film was removed, and the substrate was polished to a 40 mm long chip. Finally, the sample was annealed for 68 min by heating it at 300 °C.

4.4 Measurements

4.4.1 1.48/1.55 μm wavelength multiplexer

For the 1.48/1.55 μm wavelength multiplexer spectral transmission measurements were performed. Light from a halogen-tungsten lamp was directed through a scanning monochromator and coupled by a 40x microscope objective in the common waveguide of the multiplexer. Power from the 1.48 μm and 1.55 μm ports was collected by a 25x microscope objective and directed through a mechanical chopper to a Ge photodiode detector connected to a lock-in amplifier and a computer. Non-polarized light was used in the measurements. The measured normalized spectral transmission curves are seen in **Figure 4.2**. The pump window is centred at 1.48 μm and the signal window at 1.55 μm wavelength.

The fibre-device insertion loss was measured by coupling light with a single-mode fibre from a 1.557 μm laser diode to a common waveguide of the multiplexer, and collecting light from the 1.48 μm and 1.55 output ports to a photodetector using a 25x microscope objective. The transmission of the microscope objective was measured separately. Here, also the

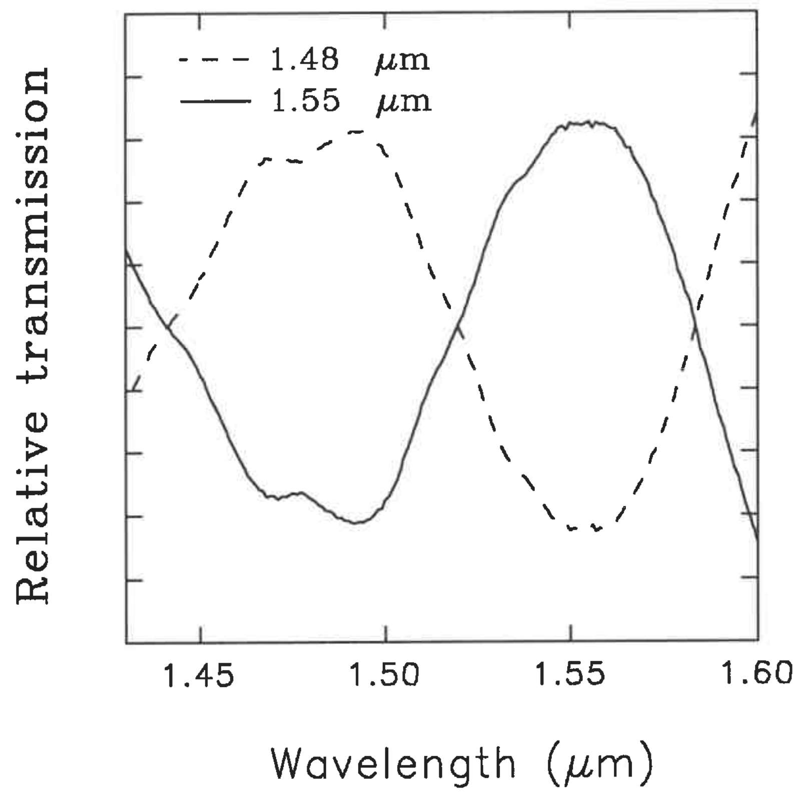

Figure 4.2 Measured spectral transmission of 1.48/1.55 μm wavelength multiplexer. Dashed and solid curves are outputs from wide and narrow arms, respectively.

crosstalk in the device, when used as a demultiplexer could be measured (which is not very important, since the device is used only as a multiplexer). The measured fibre-device insertion loss is 5.49 dB, of which about 3 dB is coupling loss and 1 dB (0.25 dB/cm) [8] is waveguide loss. Therefore, the facet-to-facet excess loss, at 1.556 μm wavelength, is less than 2.49 dB, of which about 1 dB is waveguide loss and only 1.49 dB is due to the device configuration. The measured extinction ratio at 1.556 μm wavelength is 19 dB.

4.4.2 1.30/1.55 μm wavelength multiplexer and 1/8 splitter

For the measurements of the 1.30/1.55 μm wavelength multiplexer followed by a 1/8 splitter a single-mode fibre was used to launch light separately from 1.273 μm (within 1.3 μm window) and 1.557 μm laser diodes in the respective input waveguide. The fibre-device insertion loss measurements were performed by collecting the light from the eight output ports with a microscope objective to a photodetector. The measured insertion loss (including the input fibre-chip coupling and the 8-way splitting) for each output port is shown in **Figure 4.3a** for 1.273 μm wavelength, and in **Figure 4.3b** for 1.557 μm wavelength. At 1.273 μm wavelength, the mean insertion loss is 14.65 dB with a standard deviation of 0.34 dB and a maximum deviation of 0.59 dB. At 1.557 μm wavelength the mean insertion loss is 14.48 dB with a standard deviation of 0.22 dB and

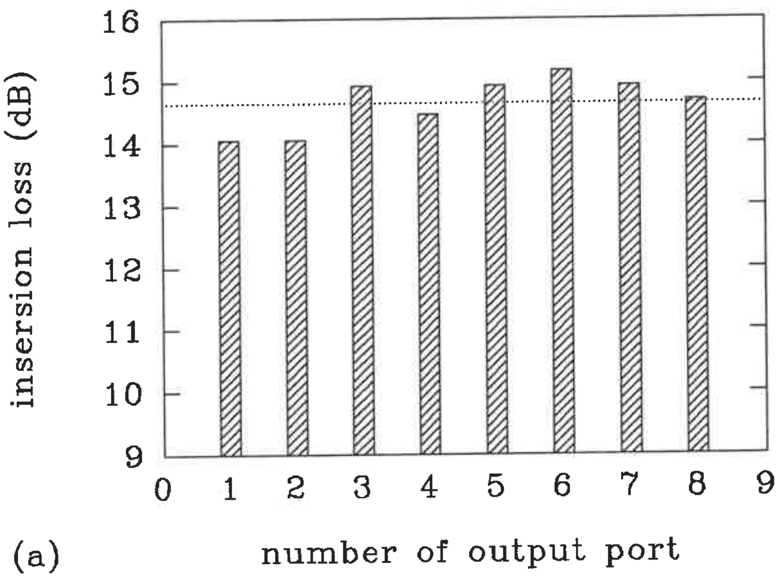

(a)

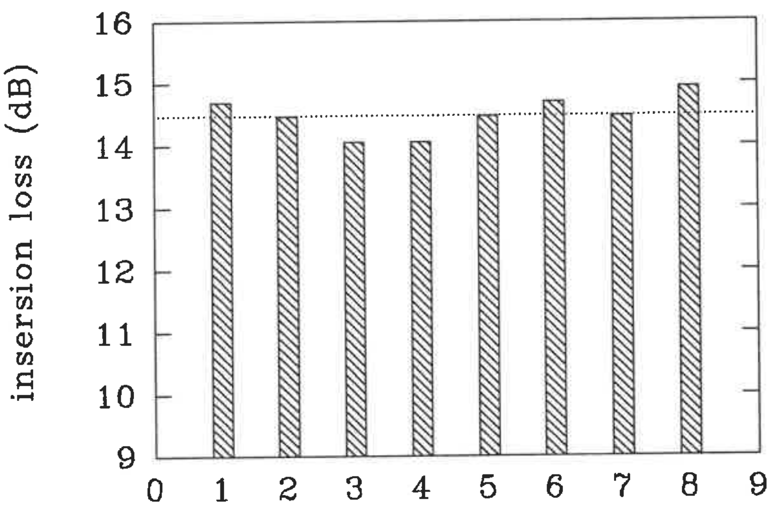

(b)

Figure 4.3. Measured fiber–chip insersion loss of the integrated 1.30/1.55 μm wavelength multiplexer and 1/8 splitter a) at 1.273 μm b) at 1.557 μm

a maximum deviation of 0.45 dB. From separate measurements at 1.273 μm wavelength of straight waveguides fabricated with similar parameters, we know that the coupling loss of these small mode size double-ion-exchanged waveguides with a fibre is over 3 dB (note that the fibre-chip coupling loss can be considerably reduced, for example, by thermally tapering [9] the input and output waveguides), and the waveguide loss is about 0.25 dB/cm. Therefore, the facet-to-facet excess loss, at both wavelengths, is less than 2.65 dB, of which about 1 dB is waveguide loss and only 1.65 dB is due to the device configuration.

4.5 Discussion and Conclusion

We have fabricated a 1.48/1.55 μm wavelength multiplexer and an integrated 1.30 μm/1.55 μm wavelength multiplexer and a 1/8 splitter in a single glass substrate by a simple double-ion exchange process. The measured facet-to-facet excess loss in the 40 mm long chip is less than 2.49 dB for the 1.48/1.55 μm multiplexer and less than 2.65 dB for the integrated multiplexer and 1/8 splitter, although we used aluminum as a masking material for ion exchange and an inexpensive multipurpose glass as a substrate. The demonstrated passive integrated optical circuit can be applied in connection with an Er-doped fibre in future WDM subscriber networks, in which amplification is needed at 1.55 μm wavelength window.

In this work we used double-ion-exchanged surface waveguides, whose single-mode region is relatively narrow. In fact, the waveguides are clearly single mode only at 1.55 μm wavelength and barely single-mode at 1.48 μm wavelength. In the 1.3 μm wavelength region the waveguides support several modes. This, however, does not cause any harm, as long as the device operates with the fundamental mode, as is the case here, when single-mode fibres are used in the inputs of the wavelength multiplexers. However, in a bidirectional WDM system, the 1.30/1.55 μm multiplexer should also operate as a wavelength demultiplexer. In this case, if light at 1.3 μm wavelength is transmitted by the subscriber, the waveguides should be single-mode also at 1.3 μm. Otherwise the behaviour of the 1.30/1.55 μm wavelength demultiplexer will be deteriorated by the higher order modes exited in Y-branch power combiners. However, it is straightforward to design our device, for example, for buried ion-exchanged glass waveguides, which are single-mode at both 1.3 μm and 1.55 μm wavelength regions.

4.6 Acknowledgement

The authors wish to thank S. Tammela and M. Tahkokorpi for fruitful discussions. This work was funded in part by a university grant from Natural Sciences and Engineering Research Council (NSERC) of Canada, and Bell Nothern Research

(BNR). The visit of S. Honkanen was funded by an International Fellowship grant from NSERC.

4.7 References

[1]. D.B. Keck, A.J. Morrow, D.A. Nolan, D.A. Thompson, "Passive components in the subscriber loop", *J. Light wave Technol*. Vol.7, pp. 1623-1633, 1989.

[2]. A. Tervonen, P. Pöyhönen, S. Honkanen, M. Tahkokorpi, "A guided-wave Mach-Zehnder interferometer structure for wavelength multiplexing", *IEEE Photon. Technol. Lett.* Vol. 3, pp. 516-518, 1991.

[3]. A. Tervonen, S. Honkanen, S.I. Najafi, "Analysis of symmetric directional coupler and asymmetric Mach-Zehnder interferometers as 1.30/1.55 μm dual wavelength demultiplexers/multiplexers", *Optical Engineering,* Vol. 32, No.9, pp. 2083-2091, 1993.

[4]. A. Tervonen, P. Pöyhönen, S. Honkanen, M. Tahkokorpi and S. Tammela, "Examination of two-step fabrication methods for single-mode fibre compatible ion-exchanged glass waveguides", *Appl. Opt*. Vol. 30, pp. 338-343, 1991.

[5]. Y. Cheng, W. Lin and Y. Fujii, "Local field analysis of bent graded-index planar waveguides", *J. Lightwave Technol*. Vol.8, pp. 1461-1469, 1990.

[6]. G. Zhang, S. Honkanen, S.I. Najafi and A. Tervonen, "1.30/1.55 and 1.48/1.55 wavelength multiplexers/ demultiplexers by double-ion exchange in glass", *OSA/ILS '93,* Toronto, 1993.

[7]. S.I. Najafi, "Waveguides and devices", chapter 6 in "Introduction to Glass Integrated Optics", Artech House, Boston, 1992.

[8]. W.J. Wang, S. Honkanen, S.I. Najafi and A. Tervonen, "New integrated optical ring resonator in glass", *Electron. Lett.*, Vol. 28, pp. 1967-1968, 1992.

[9]. A. Mahapatra and J.M. Connors, "Thermal tapering of ion-exchanged channel guides in glass", *Opt. Lett.* Vol. 3, pp. 169-171, 1988.

CHAPTER 5

CONCLUSION

In this work, a 1.48/1.55 μm wavelength division multiplexer and 1.30/1.55 μm wavelength division multiplexer and a 1/8 splitter are produced in a single glass substrate by a simple (potassium and silver) double ion-exchange process. The operation of these WDM and splitter devices has been successfully demonstrated.

In Chapter 2, the integrated 1.30/1.55 μm WDM and a 1/8 splitter was described. This device was fabricated in a single glass substrate by a simple double ion-exchange process. The measured facet-to-facet excess loss in the 40 mm long chip was less than 2.5 dB, although we used aluminium as a masking material for ion exchange, and an inexpensive multipurpose glass as the substrate. The deviation among the 8 outputs was very small.

In Chapter 3, the effect of post-annealing on the optical behaviour of the 1.30/1.55 μm and 1.48/1.55 μm three-port integrated optics Mach-Zehnder interferometer in glass for multi/demultiplexer applications was investigated. It was found that the overall spectral characteristics of the 1.30/1.55 μm device were little sensitive to post-annealing. The centre wavelength of "stop band" remains the same. On the contrary, the spectral characteristics of the 1.48/1.55 μm device are sensitive to post-annealing. This effect can be employed positively for fine-tuning of the optical characteristics of these devices after fabrication is completed.

In Chapter 4, the integration of a 1.48/1.55 μm WDM and an integrated optics 1.30/1.55 μm WDM followed by a 1/8 splitter was demonstrated. This device was also fabricated in a single glass substrate by a simple double ion-exchange process. The measured facet-to-facet excess loss in the 40 mm long chip was less than 2.49 dB for the 1.48/1.55 μm WDM and less than 2.65 dB for the integrated 1.30/1.55 μm WDM and 1/8 splitter. The demonstrated passive integrated optical circuit can be applied in connection with an Er-doped fibre in future WDM subscriber networks, in which amplification is needed at 1.55 μm wavelength window.

With respect to future work, there are a number of interesting applications based on the demonstration of the passive devices in this thesis.

In this thesis, we used double ion-exchanged surface waveguides, whose single-mode region is relatively narrow. In fact, the waveguides are clearly single mode only at 1.55 μm wavelength, and barely single-mode at 1.48 μm wavelength. At 1.30 μm wavelength region the waveguides support several modes. In a bidirectional WDM system, the 1.30/1.55 μm wavelength multiplexer should operate also as a wavelength demultiplexer. In this case, if light at 1.30 μm is transmitted by the subscriber, the waveguides should be single-mode also at 1.30 μm. Otherwise the behaviour of the 1.30/1.55 μm WDM will be deteriorated by higher order modes excited in Y-branch power combiners. In order to solve this problem, we can design the device for buried ion-exchanged glass waveguides, which are single-mode in both 1.30 and 1.55 μm wavelength regions.

In the future WDM networks, there is also a need to amplify the 1.30 μm signal light. If Nd-fibre is used, we can design and fabricate 0.807/1.30 μm WDM where 0.807 μm wavelength is used as the pump wavelength. Then, the 1.3/1.55 μm WDM can be employed to multiplex the two amplified signals.

References

[1]. ALBERT J., WANG W. J. and S. I. NAJAFI, "Optical damage threshold of ion-exchanged glass waveguides at 1.06 μm", *Conference on Integrated Optics Circuits,* Paper #4, Boston, 1991.

[2]. CHENG Y., LIN W. and FUJII Y., "Local field analysis of bent graded-index planar waveguides", *J. Lightwave Tech.*, Vol. 8, pp. 1461-1469, 1990.

[3]. IZAWA T. and NAKAGOME H., "Silver ion-exchanged glass waveguides", *Appl. Phys. Lett.,* Vol. 21, pp. 584-586, 1972.

[4]. HEJMERS H., HELLESO O. G., BENECH P., and RIMET R., "Single mode potassium and silver ion-exchanged glass waveguides with low losses and high index increase", *Appl. Phys. Lett.*, pp. 2759-2760, 1992.

[5]. KAPON E. and THURSTON R. N., "Multichannel waveguide junctions for guide-wave optics", *Appl. Phys. Lett.*, Vol. 50, No. 24, pp. 1710-1712, 1987.

[6]. KECK D. B., MORROW A. J., NOLAN D. A., and THOMPSON D. A., "Passive components in the subscriber

loop", *J. Lightwave Technol.*, LT-7, pp. 1623-1633, 1989.

[7]. LI M. J., HONKANEN S., LEONELLI R., Albert J. and Najafi S. I., *Appl. Phys. Lett.*, pp. 2607-2609, 1991.

[8]. MAHAPATRA A., and CONNORS J. M., "Thermal tapering of ion-exchanged channel guides in glass", *Opt. Lett.*, 3, pp.169-171, 1988.

[9]. MILLER. S. E., "Integrated optics: an introduction", *Bell Sys. Tech. J.*, Vol. 48, pp. 2056-2068, 1969.

[10]. NAJAFI S. I., "Introduction to Glass Integrated Optics", Artech House, Boston, 1992.

[11]. NAJAFI S. I., "Critical Review Conference on Integrated Optics and Optoelectronics", Jan. 1993, invited paper, *SPIE Proceeding* #CR45, pp. 358-368, 1993.

[12]. NISHIHARA H., HARUNA M. and SUHARA T., "Optical integrated circuits", Mcgraw-Hill, New York, 1989.

[13]. NISSIM C., BEGUIN A., LABORDE P., LERMINAUX C. and McCourt M., *Proc. EFOC/LAN 90*, 27-29 June 1990,

Munich, IGI Europe 1990, pp. 114-116.

[14]. OKUDA E., TANAKA I. and YAMASAKI T., "Planar gradient-index glass waveguide and its applications to a 4-port branched circuits and star coupler", *Appl. Opt.*, Vol. 3, pp. 1745-1748, 1984.

[15]. REICHELT A. H., CLEMENS P. C. and MAHLEIN H.F., *Proc. SPIE 1128*, pp. 165-168, 1989.

[16]. SAARINEN J., HUTTUNEN J., HONKANEN S., NAJAFI S. I. and TURUNEN J., "Computer-generated waveguide holograms by double ion-exchange process in glass", *Electron. Lett.*, Vol. 28, No.9, pp. 876-878, 1992.

[17]. SANFORD N. A., MALONE K. J., LARSON D. R. and HICKEMELL R. K., "Y-branch waveguide glass laser and amplifier", *Opt. Lett.*, Vol. 16, pp. 1168-1170, 1991.

[18]. TERVONEN A., PÖYHÖNEN P., HONKANEN S., and TAHKOKORPI M., "A guided-wave Mach-Zehnder interferometer structure for wavelength multiplexing", *IEEE Photonics Technol. Lett.*, pp. 516-518, 1991.

[19]. TERVONEN A., PÖYHÖNEN P., HONKANEN S., TAHKOKORPI M., and TAMMELA S., "Examination of two-step fabrication

methods for single-mode fibre compatible ion-exchanged glass waveguides", *Appl. Opt.*, pp. 338-343, 1991.

[20]. TERVONEN A., HONKANEN S. and NAJAFI S. I., "Analysis of symmetric directional couplers and asymmetric Mach-Zehnder interferometers as 1.30/1.55 μm dual wavelength demultiplexers/ multiplexers", *Optical Eng.*, Vol. 32, pp. 2083-2091, 1993.

[21]. TTEYZ G. V., "Silicon Mach-Zehnder waveguide interferometer operating at 1.30 μm", *Electron. Lett.*, Vol. 27, pp. 118-120, 1991.

[22]. VILJANEN J. and LEPPIHALME M., "Analysis of loss in ion-exchange glass waveguides", *Proc. 1st Eur. conf. Integrated Optics*, pp.18, 1981.

[23]. WALKER R. G., WILKINSON C. D. W. and WILKINSON J. A. H., "Integrated optical waveguiding structures made by silver ion-exchange in glass: 1. The propagation characteristics of strip ion-exchanged waveguides; a theoretical and experimental investigation", *Appl. Opt.*, Vol. 22, pp. 1923-1928, 1983.

[24]. WANG W. J., HONKANEN S., NAJAFI S. I. and TERVONEN

A., "New integrated optical ring resonator in glass", *Electron. Lett.*, Vol. 28, pp. 1967-1968, 1992.

[25]. Wang W. J., HONKANEN S., NAJAFI S. I.and TERVONEN A. J. *Appl. Phys.*, pp. 1529-1533, 1993.

[26]. ZHANG G., HONKANEN S., NAJAFI S. I. and TERVONEN A., "1.30/1.55 and 1.48/1.55 wavelength multiplexers/ demultiplexers by double-ion exchange in glass", *OSA/ILS '93,* Toronto, 1993.